Interventions to improve mitochondrial function in a mouse model of GRACILE syndrome, a complex III disorder

Jayasimman Rajendran

Folkhälsan Research Center

and

Doctoral Program in Biomedicine
Pediatrics, Faculty of Medicine,
University of Helsinki

Academic Dissertation

To be presented, with permission from the Faculty of Medicine at the University of Helsinki, for public examination in the Lecture Hall 2, Haartman Institute, Haartmaninkatu 3, Helsinki on 5th April 2019 at 12 noon

Helsinki 2019

Supervisors:

Vineta Fellman, M.D. Ph.D., Professor
Folkhälsan Research Center
Biomedicum, P.O.Box 63 (Haartmaninkatu 8), FI-00014, Finland.
Lund University, Department of Clinical Sciences, Lund,
Pediatrics, Lund University, Sweden.

Jukka Kallijärvi, Ph.D., Docent
Folkhälsan Research Center
Clinicum, University of Helsinki
Biomedicum, P.O.Box 63 (Haartmaninkatu 8), FI-00014, Finland.

Thesis Advisory Committee:

Alberto Sanz, Ph.D., Principal Research Associate
Ageing Research Laboratories, Institute for Cell and Molecular Biosciences
Newcastle University, Campus for Ageing and Vitality
Newcastle upon Tyne, NE4 5PL,UK.

Henna Tyynismaa, Ph.D., Docent Associate Professor
Research Program for Molecular Neurology, University of Helsinki
Biomedicum, P.O.Box 63 (Haartmaninkatu 8), FI-00014, Finland.

Reviewers:

Alexander Kastaniotis, Ph.D., Docent
University Researcher, Group Leader
Faculty of Biochemistry and Molecular Medicine
P.O.Box 5400, FIN-90014 University of Oulu, Finland

Riikka Martikainen, Ph.D., Docent
University of Eastern Finland
A.I.Virtanen Institute for Molecular Sciences,
P.O.Box 1627 (Neulaniementie 2), FI-70211 Kuopio, Finland.

Opponent:

Cristina Ugalde, Ph.D., Professor
Instituto de Investigación Hospital,
12 de Octubre (i+12), Madrid 28041, Spain
Centro de Investigación Biomédica en Red de Enfermedades Raras (CIBERER),
U723, Madrid 28029, Spain

ISBN 978-951-51-4947-3 (Paperback)
ISBN 978-951-51-4948-0 (PDF)
http://ethesis.helsinki.fi

Unigrafia Oy
Helsinki 2019

நோய்நாடி நோய்முதல் நாடி அதுதணிக்கும்
வாய்நாடி வாய்ப்பச் செயல்

(Diagnose the illness, trace its cause, seek the proper remedy and apply it with skill)

- திருவள்ளுவர் (Triuvalluvar)

திருக்குறள்-948 (Tirukkural-948) | Dated 300 BCE

Content

List of original publications

I. **Rajendran J**, Tomasic N, Kotarsky H, Hansson E, Velagapudi V, Kallijärvi J, Fellman V. Effect of high-carbohydrate diet on plasma metabolome in mice with mitochondrial respiratory chain complex III deficiency. *Int J Mol Sci* 2016;17:1824; DOI:10.3390/iijms17111824

II. Purhonen J, **Rajendran J**, Mörgelin M, Uusi-Rauva K, Katayama S, Krjutskov K, Einarsdottir E, Velagapudi V, Kere J, Jauhiainen M, Fellman V, Kallijärvi J. Ketogenic diet attenuates hepatopathy in mouse model of mitochondrial respiratory chain complex III deficiency caused by a *Bcs1l* mutation. *Sci Rep* 2017;7:957; DOI:10.1038/s41598-017-01109-4

III. **Rajendran J**, Purhonen J, Tegelberg S, Smolander OP, Mörgelin M, Rozman J, Gailus-Durner V, Fuchs H, Hrabe de Angelis M, Auvinen P, Mervaala E, Jacobs HT, Szibor M, Fellman V, Kallijärvi J. Alternative oxidase-mediated respiration prevents lethal mitochondrial cardiomyopathy. *EMBO Mol Med* 2018; e9456; DOI 10.15252/emmm.201809456

In the text, the publications are referred to by their Roman numbers. Additional unpublished results are included. All the published articles are reprinted with the permission of copyright owners.

Contributions:

I. I performed metabolomics data analysis, interpreted the results and prepared image panels and wrote the manuscript.

II. I participated in the study design, carried out the animal experiments, performed phenotyping, collected samples, and analyzed plasma metabolomics data.

III. I carried out the animal experiments including breeding, genotyping, examination of animal health, echocardiography, CLAMS, and metabolic cage. I sacrificed animals, collected tissues and did laboratory experiments as follows: histology, protein analyses by Western Blotting, BNGE, isolated mitochondrial respirometry, mitochondrial CIII activity. I analyzed the data for metabolomics and transcriptomic studies. I participated in designing and writing the manuscript.

Abbreviations

ADP	adenosine diphosphate
AIF	apoptosis-inducing factor
AMP	adenosine monophosphate
ANOVA	analysis of variance
AOX	alternative oxidase
ATF3	activating transcription factor 3
ATF4	activating transcription factor 4
ATP	adenosine triphosphate
BCAA	branched-chain amino acids
BNGE	blue native gel electrophoresis
bp	base pair
BSA	bovine serum albumin
cAMP	cyclic adenosine monophosphate
CD68	cluster of differentiation 68
CLAMS	comprehensive lab animal monitoring system
Complex I (CI)	reduced nicotinamide adenine dinucleotide dehydrogenase
Complex III (CIII)	succinate dehydrogenase
Complex IV (CIV)	cytochrome c oxidase
COX	cytochrome c oxidase
CS	citrate synthase
DEXA	dual-energy X-ray absorptiometry
DMSO	dimethyl sulphoxide
DNA	deoxyribonucleic acid
EDTA	ethylenediamine tetraacetic acid
EF	ejection fraction
EGTA	ethylene glycol-bis-(β-aminoethyl ether)-N,N,N',N'-tetraacetic acid
eNOS	endothelial nitric oxide synthase
ETC	electron transport chain
ETFAα	electron transport flavoprotein alpha-polypeptide
FAD	flavin adenine dinucleotide
FADH2	reduced flavin adenine dinucleotide
FCCP	carbonyl cyanide-4-(trifluoromethoxy) phenylhydrazone
FDR	false discovery rate
FS	fractional shortening
GABA	gamma-aminobutyric acid
GFAP	glial fibrillary acidic protein
GFP	green fluorescent protein
GMC	German Mouse Clinic
GRAC	homozygous *Bcs1l*$^{c.A232G}$ mouse
GROX	homozygous *Bcs1l*$^{c.A232G}$ mouse expressing AOX
GSH	reduced glutathione
GSSG	oxidized glutathione
H&E	hematoxylin and eosin staining

HCD	high carbohydrate diet
HEPES	2-[4-(2-hydroxyethyl)piperazin-1]-ethanesulfonic acid
HIF-1α	hypoxia-inducible factor 1-alpha
HNE	4-hydroxy-2-nonenal
HRP	horseradish peroxidase
IBA1	allograft inflammatory factor 1
IMM	inner mitochondrial membrane
IMS	intermembrane space
iNOS	inducible nitric oxide synthase
KD	ketogenic diet
KYN	kynurenine
KYNA	kynurenic acid
LV Vol;D	left ventricule volume at diastolic state
LV Vol;S	left ventricule volume at systolic state
MDA	malondialdehyde
MHC	major histocompatibility complex
mRNA	messenger ribonucleic acid
MS	mass spectrometry
mtDNA	mitochondrial deoxyribonucleic acid
NAD^+	nicotinamide adenine dinucleotide (oxidized)
NADH	nicotinamide adenine dinucleotide (reduced)
NADP	nicotinamide adenine dinucleotide phosphate
nDNA	nuclear deoxyribonucleic acid
NDUFS	NADH dehydrogenase ubiquinone iron-sulphur
NDUFV1	NADH dehydrogenase
nNOS	neuronal nitric oxide synthase
NO	nitric oxide
NOS	nitric oxide synthase
nPG	n-propyl gallate
$O_2^{\cdot -}$	superoxide anion
ORO	Oil Red O
OXPHOS	oxidative phosphorylation
PAS	periodic acid–Schiff
PBS	phosphate-buffered saline
PCA	principle component analysis
PCR	polymerase chain reaction
PDH	pyruvate dehydrogenase
PDHE1a	pyruvate dehydrogenase E1
PGC-1α	peroxisome proliferator-activated receptor (PPAR) gamma coactivator -1α
PMSF	phenylmethanesulfonyl fluoride
POLG	polymerase gamma (γ)
PPAR	peroxisome proliferator-activated receptor
PVDF	polyvinylidene fluoride
Q	ubiquinone
QH_2	ubiquinol

RC	respiratory chain
RISP	Rieske iron-sulfur protein
RNA	ribonucleic acid
RNS	reactive nitrogen species
ROS	reactive oxygen species
rRNA	ribosomal ribonucleic acid
S1BF	somatosensory cortex barrel field
SC	supercomplex
SD	standard deviation
SDHB	succinate dehydrogenase complex iron-sulfur subunit B
SDS	sodium dodecyl sulfate
SMA	smooth muscle alpha-actin
SOD	superoxide dismutase
SUIT	substrate uncoupler inhibitor titration
TBARS	thiobarbituric acid reactive substances
TBS	TRIS buffered saline
TCA	tricarboxylic acid cycle
TFAM	mitochondrial transcription factor A
TMPD	N,N,N′,N′-tetramethyl-p-phenylenediamine
TNF-alpha	tumor necrosis factor alpha
UCP1	uncoupling protein 1
v/v	volume per volume
VDAC1	voltage-gated ion channel 1
w/v	weight per volume
w/w	weight per weight
WT	wild-type

Abstract

A rare homozygous *BCS1L*$^{c.A232G}$ (Ser78Gly, p.S78G) mutation in infants causes GRACILE syndrome, which is a severe mitochondrial respiratory chain complex III (CIII) disorder resulting in multiple organ dysfunction and early lethality. Pathogenesis mechanisms have been studied using our viable *Bcs1l*$^{p.S78G}$ knock-in mouse model. The mouse model replicates most clinical phenotypes, such as growth restriction, hepatopathy, and tubulopathy. Like patients, the survival of homozygous mice is reduced (to 35-45 days, P35-P45 in the C57BL/6JBomTac background), mainly because of severe hypoglycemia. Aiming to improve the glycemic balance we performed an intervention with a high sugar (60% dextrose) diet. This diet did not improve energy metabolism and resulted in slightly decreased survival despite apparent normalization of some plasma metabolites.

For subsequent studies, we bred the *Bcs1l*$^{c.A232G}$ mutation into a C57BL/6JCrl background, in which the survival was five-fold longer (approximately 200 days). Moreover, the extended survival brought novel phenotypes, such as encephalopathy and late-onset cardiomyopathy. In this genetic background, we investigated the effect of ketogenic diet on disease progression. The ketogenic diet had a beneficial impact on liver disease, but it had adverse effects upon long-term feeding, resulting in shortened survival. In the third study, we introduced an alternative oxidase (AOX) transgene into the *Bcs1l*$^{p.S78G}$ mice to improve respiratory chain function. The ubiquitous expression of AOX, which should bypass electron transfer and relieve CIII blockade, prevented lethal cardiomyopathy and renal-tubular atrophy, and delayed focal astrogliosis in the somatosensory cortex of the brain. The beneficial effects of AOX extended the median survival of the homozygotes to median P590.

The main conclusions from these studies are that the *Bcs1l*$^{p.S78G}$ mice in a C57BL/6JCrl background present with both the known early-onset manifestations of GRACILE syndrome and some later-onset manifestations found in other CIII deficiencies. The dietary interventions had limited benefits, probably because of a severe course of the disease. In contrast, bypassing the blocked electron flow using AOX had a robust beneficial effect, mainly in tissues or cells with high ATP demand such as the heart and renal proximal tubular cells.

1 Introduction

Mitochondrial disorders are common inborn errors of metabolism and vary widely in their presenting age and symptoms. The genetic cause may be an inherited or acquired mutation(s) either in the nuclear DNA (nDNA) or mitochondrial DNA (mtDNA). The products of more than 1000 genes encoded in nDNA and 37 genes in mtDNA play a role in both biogenesis and functions of mitochondria, including mitochondrial respiration by the respiratory chain (RC) complexes. Furthermore, a specific mutation in either genome can cause mitochondrial dysfunction which results in a wide range of diseases and pathological conditions.

With the current developments in clinical diagnostics, including advanced molecular genetics, it is often possible to identify the causative mutation(s) of disease. However, effective treatments are currently not available for mitochondrial disorders, despite several promising drugs that affect various energy-metabolism pathways in RC deficiency. To develop effective therapeutic strategies, detailed knowledge of disease mechanisms is necessary.

This thesis work is based on the need to understand disease mechanisms in GRACILE syndrome, which is by far the most severe RC complex III (CIII) disorder (Fellman *et al.* 1998). Its cause is a homozygous *c.A232G* mutation in nuclear DNA gene encoding BCS1L, which is an assembly factor for CIII. This mutation changes a single amino acid (serine 78 to glycine) in the protein (Visapää *et al.* 2002), which in turn affects CIII assembly. The resulting typical phenotype consists of severe fetal Growth Restriction, Aminoaciduria, due to Fanconi type proximal tubulopathy, Cholestasis, Iron accumulation, Lactic acidosis, and Early death during infancy, the base for the acronym (Fellman *et al.* 1998, Visapää *et al.* 2002). The particular genotype-phenotype consistency in infants (Fellman *et al.* 2008) motivated Professor Fellman's group to generate a mouse model by introducing the patient mutation into the mouse genome (Levéen *et al.* 2011). It resulted in the first viable mouse model for CIII deficiency, mimicking the human disease, but with an initial symptom-free postnatal period. Breeding the mutation into the C57BL/6JCrl background at the University of Helsinki resulted in longer survival and additional phenotypes. We used both mouse strains for investigations in this thesis with the aim to describe mechanisms and assess the efficacy of therapeutic interventions.

2 Review of the literature

2.1 The origin and structure of mitochondria

Mitochondria are double membrane-bound organelles that generate ATP using aerobic respiration and also participate in the signaling pathways for cell cycle, differentiation, and death (McBride *et al.* 2006). The current widely-accepted theory about the origin of the mitochondrion is the endosymbiont theory. It posits that an archaeon engulfed an alpha-proteobacterium in building a symbiotic relationship, resulting in a primitive eukaryotic cell (Martin *et al.* 2015). Unlike other organelles, mitochondria function through proteins encoded both in the nucleus and mitochondrial DNA (mtDNA). Mammalian mitochondria have double-stranded circular mtDNA consisting of 15-17 kbp with a heavy strand (guanine-rich) containing 28 genes and a light strand (cytosine-rich) with 9 genes. Of these 37 genes, 22 encode transfer RNA, 2 encode ribosomal RNA, and 13 encode polypeptides, which are subunits of mitochondrial respiratory complexes (Taanman 1999).

The mtDNA is present in the internal space called the matrix that is abundant with enzymes, peptides, and proteins, which play a role in the metabolic processes such as pyruvate and fatty acid oxidation, and tricarboxylic acid (TCA) cycle. The matrix is enclosed by two phospholipid bilayers. They is an inner mitochondrial membrane (IMM) and an outer mitochondrial membrane (OMM), separated by an inter-membrane space (IMS). The OMM maintains the integrity of the mitochondrion structure and separates inner contents from the cytosol. The OMM contains various enzymes involved in metabolic processes (e.g., fatty acid elongation) (Howard 1970) and membrane transport. Transportation of large proteins occurs directly by translocase proteins, and small molecules such as ions and ATP (<5 kDa) pass through the channels and transporters (i.e., porin) (Endo & Kohda 2002). The IMM folding forms the cristae that provide space for the IMM-located enzymes and proteins to enhance RC complex activity (Bartolák-Suki *et al.* 2017).

2.1.1 Mitochondria in ATP generation

One of the many important functions of mitochondria is ATP synthesis, mainly by the IMM-located ATP synthase (complex V, CV). The CV requires a proton gradient generated by electron transfer through RC complexes. The RC complexes are NADH dehydrogenase (complex I, CI), succinate dehydrogenase (complex II, CII), cytochrome c reductase (complex III, CIII), and cytochrome c oxidase (complex IV, CIV). These RC complexes exist either in free form or are combined to form so-called supercomplexes (SC) such as $CI/III_2/IV$, CI/III_2, and $CIII_2/IV_n$ (Schägger 2001). They are involved in the proton pumping into the IMS and maintain the gradient (Guo *et al.* 2018) (Figure 1).

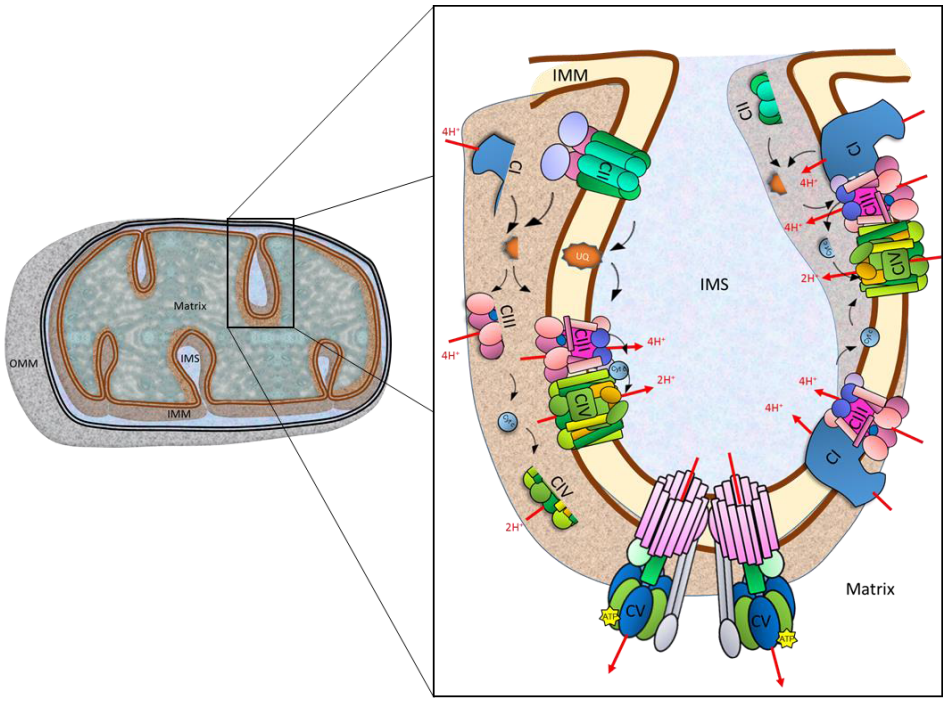

Figure 1. Schematic structure of the mitochondrion and the respiratory chain complexes in the IMM. IMM, inner mitochondrial membrane; IMS, intermembrane space; OMM, outer mitochondrial membrane; CI, complex I; CII, Complex II; CIII, Complex III; CIV, Complex IV; CV, ATP synthase; UQ, ubiquinol. Red arrows indicate proton translocation, while black arrows indicate the direction of electron transfer. Individual RC complex structures in this figure are redrawn based on the image provided for the KEGG project by Kanehisa Laboratories.

Complex I oxidizes NADH, which is a product of pyruvate oxidation and TCA cycle. CI releases four protons into the IMS and transfers two electrons to reduce ubiquinone (Q), also known as coenzyme Q_{10}. CI consists of 45 subunits, among them seven (ND1–ND6 and ND4L) are mtDNA-encoded proteins forming the major part of the membrane domain (Hirst *et al.* 2003; Mimaki *et al.* 2012), which is involved in proton translocation and ubiquinone binding (Hoogenraad *et al.* 2002; Hirst *et al.* 2003). The additional 38 subunits are nDNA-encoded proteins, of which seven subunits (NDUFV-2, NDUFS1-3, and NDUFS7-8) form the core that oxidizes NADH and initiates electron transfer (Vogel *et al.* 2007; Lazarou *et al.* 2009). The remaining 31 subunits contribute to the structural stability and biogenesis of CI (Friedrich & Böttcher 2004; Mimaki *et al.* 2012). Complex II is not bound to any other complexes and consists of four nDNA-encoded core subunits, (SDH-A-D). It dehydrogenates succinate to fumarate, part of the TCA cycle, and transfers electrons to Q without proton transfer to the IMS (Cecchini 2003; Ylikallio & Suomalainen 2012).

Complex III consists of 10 subunits, of which cytochrome b is mtDNA-encoded, and the rest are nDNA-encoded. CIII receives electrons from ubiquinol (QH_2) and, transfers them to reduce two molecules of cytochrome c, with concomitant translocation of four protons into the IMS (Fernandez-Vizarra & Zeviani 2018). Complex IV contains 13 subunits. Three mtDNA-encoded proteins are large core subunits (COX1-3) responsible for electron transfer. The other ten nDNA-encoded subunits stabilize the complex and regulate the biogenesis. CIV re-oxidizes cytochrome c and releases two protons into the IMS and converts oxygen molecules into water (Fernández-Vizarra *et al.* 2009).

In summary, the RC complexes carry out mitochondrial respiration to meet the ATP demand of the cell. Impairment of RC complexes disrupts the electron transport chain (ETC) and proton translocation, which in turn impairs mitochondrial ATP synthesis (Shi *et al.* 2008; Xiao *et al.* 2014). Furthermore, ETC disruption can have an indirect impact on metabolic pathways such as glycolysis, fatty acid oxidation and the TCA cycle (Zieliński *et al.* 2016). As the TCA cycle is driven by acetyl-CoA from either glycolysis or fatty-acid oxidation to produce NADH and $FADH_2$ for CI and CII activity, respectively, impairment of the ETC can inhibit the TCA cycle.

2.2 CIII assembly and function

Cryo-EM analysis (Guo *et al.* 2018) shows CIII in IMM as a tightly packed dimer. Its assembly begins with the synthesis of the mtDNA-encoded cytochrome b (CYTB), followed by incorporation of nDNA-encoded subunits. The translation factors UQCC1 and UQCC2 bind to CYTB and help to stabilize the complex structure during insertion into the IMM. There, bL heme binds to CYTB followed by UQCC3, which releases UQCC1 and UQCC2 from their binding. Sequential incorporation of bH heme and cytochrome c1 (CYC1) forms the pre-$CIII_2$ dimer into which Rieske iron-sulfur protein (RISP) and QCR10 get inserted (Fernandez-Vizarra & Zeviani 2018). The RISP precursor is synthesized in the cytosol and translocates through TOM and TIM23 into the mitochondrial matrix (Wasilewski *et al.* 2017). There, a matrix-processing peptidase cleaves part of the mitochondrial-transfer sequence (MTS) from the RISP molecule. A LYR-motif-containing chaperone (MZM1L/LYRM7) binds to it and recruits the Fe-S transfer complex to form a 2Fe-2S cluster (Maio *et al.* 2014; Maio *et al.* 2017). Thereafter, BCS1L translocates RISP across the IMM and incorporates it into the pre-$CIII_2$ (Cruciat et al. 1999; Wagener et al. 2011). TTC19 (Ghezzi *et al.* 2011) which binds to $CIII_2$ was recently shown to facilitate the removal of the remaining MTS from RISP to activate CIII catalytic function (Fernandez-Vizarra & Zeviani 2018).

In the fully assembled $CIII_2$, CYTB, cytochrome c1 (CYC1), and RISP are involved in electron transfer by the Q cycle (Figure 2a). CYTB has two Q binding sites (quinone oxidation Q_o, and quinone reduction Q_i sites) and two b-type hemes (bL and bH) (Fernandez-Vizarra & Zeviani 2018). Electron transfer is initiated from the binding of QH_2 and Q at Q_o and Q_i sites of CYTB, respectively. In the Q_o site, oxidation of QH_2 releases one electron to RISP and subsequently another electron to the bL heme of CYTB, accompanied by protonation of His182 of RISP, and Glu272 of CYTB (Figure 2b) (Palsdottir *et al.* 2003). The head domain of RISP releases the proton from His182 to IMS and transfers an electron to CYC1. CYC1 transfers the electron further to cytochrome c (CYTC), after which CYTC dissociates from $CIII_2$. The proton from Glu272 of CYTB is released to IMS through bL heme with the help of a water molecule. Simultaneously, an electron from bL heme is transferred via bH heme of CYTB further to Q_i site to reduce Q. A single electron will partially reduce Q to semiquinone (Figure 2b) (Palsdottir *et al.* 2003; Crofts *et al.* 2017). For complete reduction, the semiquinone acquires another electron which can be generated by another cycle of QH_2 oxidization at the Q_o site. The complete reduction of Q in Q_i takes 2 protons from the matrix. This second cycle of electron transfer reduces the second CYTC and releases two more protons into IMS (Crofts *et al.* 2017).

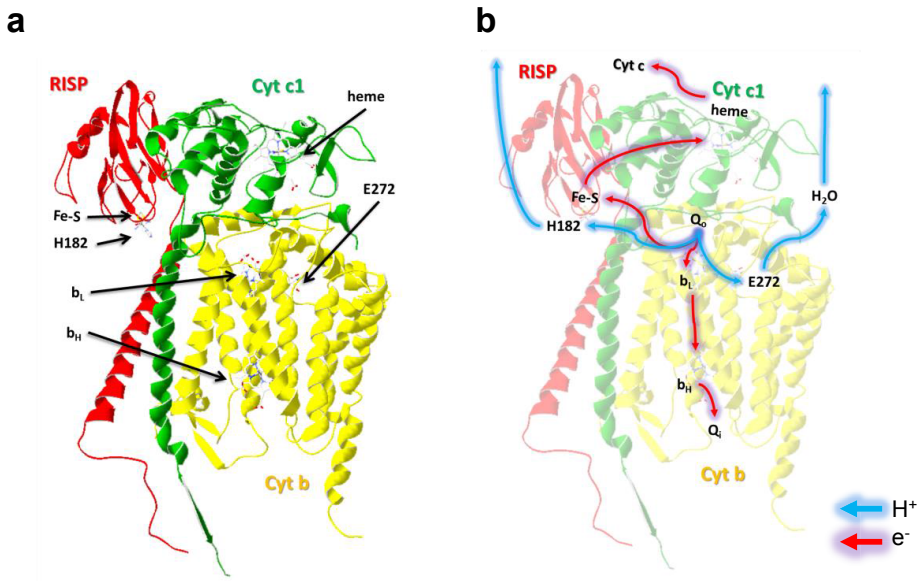

Figure 2. Crystal structure of yeast cytochrome bc_1 complex subunits. a) The tertiary structure of CIII subunits (Cytb-cytochrome b, Cyt c1-cytochrome C1, and RISP- Rieske Fe-S protein) and their heme clusters. b) Direction of proton and electron transfer in CIII subunits. The structure was obtained from the protein data bank (PDB.ID:1KYO).

2.3 Respiratory chain dysfunction

Mutations in genes encoding RC subunits lead to RC deficiencies. CI deficiency occurs in patients with homozygous or compound heterozygous mutations in genes encoding functional subunits (Lazarou *et al.* 2009), supernumerary subunits, (NDUFS4, S6, NDUFA1-2, and NDUFA10-12) (van den Heuvel *et al.* 1998; Kirby *et al.* 2004; Fernandez-Moreira *et al.* 2007; Berger *et al.* 2008; Hoefs *et al.* 2008; Hoefs *et al.* 2011), and assembly factors (NDUFAF1-5). The clinical manifestations of CI deficiency are diverse, from cardiomyopathy to Leigh syndrome (LS), which is a severe neurometabolic disorder with early lethality (Mimaki *et al.* 2012)**.** Mutations in CII subunits (SDHA-D) and assembly factors (SDHAF1-2) cause LS (Hes *et al.* 2010) and paragangliomas (Solis *et al.* 2009; Hoekstra & Bayley 2013). Mutations affecting CIII are rare and mostly in the *CYTB* gene (Barel *et al.* 2008) or assembly factors such as TTC19 (Ghezzi *et al.* 2011; Mordaunt *et al.* 2015) and BCS1L. The number of *BCS1L* mutations discovered in patients is more than 20, and they cause a wide range of clinical phenotypes (Table 1). Mutations in nDNA-encoded subunits of CIV, assembly factors (COX10, COX15, and Surf1) (Zhu *et al.* 1998; Antonicka *et al.* 2003a and 2003b), translator activating factor (TACO1) (Weraarpachai *et al.* 2009), and FAST kinase domain-containing protein (FASTKD2) (Ghezzi *et al.* 2008) can cause a wider spectrum of mitochondrial disorders, including LS or Leigh-like diseases, cardiomyopathy, and liver failure.

2.3.1 Reactive oxygen species production in mitochondria

Reactive oxygen species (ROS) are partially reduced oxygen molecules, such as superoxide, hydroxyl radical, and singlet oxygen. In mitochondria, electrons can leak from CI and CIII to oxygen, which turns into superoxide (O_2^-). Superoxide dismutase (SOD) metabolizes superoxides further into hydrogen peroxide (H_2O_2) (Jastroch *et al.* 2010). Mitochondrial ROS production generally depends on the proton motive force, the ratio of $NADH/NAD^+$ and QH_2/Q, as well as the oxygen concentration (Murphy 2009). Therefore, defective RC function can increase electron leak, which results in increased ROS production.

ROS are involved in the signaling of cell proliferation or apoptosis, depending on their level (Schieber & Chandel 2014). A mild increase in ROS regulates cysteine residues and kinases such as Akt, ERK1/2, PKA/PKC, JNK, and p38MAPK (Son *et al.* 2011; Antico Arciuch *et al.* 2012), which can induce the cell anti-apoptotic and proliferation pathways. In contrast, high levels of ROS induces cytochrome c release to the cytosol (Ames 1983), which triggers the caspase cascade for apoptosis (Ozben 2007).

2.4 BCS1L assembly factor

BCS1L, a member of the AAA-ATPases superfamily, consists of 419 amino acids. The protein 3D structure has not been solved, but sequence analysis shows three major domains: The N-terminal domain (first 126aa) containing the signal for the mitochondrial targeting and protein sorting, followed by a specific domain for activity and stability (Nouet *et al.* 2009), and the final C-terminal domain (last ~200aa) with two motifs. These two motifs play a role in the substrate binding, unfolding, and translocation (Cruciat *et al.* 1999; Wagener *et al.* 2011). BCS1L has features of AAA-ATPases, which form an oligomeric ring (hexadecamer) structure with a central pore. According to studies in yeast, the AAA-domain of the corresponding protein, Bcs1, interacts with RISP in the matrix and translocate RISP through its central pore to assemble with pre-$CIII_2$. The translocation occurs with ATP hydrolysis (Wagener & Neupert 2012).

2.4.1 Mutations in *BCS1L*

More than twenty recessive disease-causing *BCS1L* mutations have been reported. They are either as compound heterozygous or homozygous resulting in various clinical phenotypes. The most severe phenotype is the neonatal GRACILE syndrome in the Finnish population (Fellman *et al.* 1998; Fellman *et al.* 2008). Patients with GRACILE-like diseases are also found with ancestors from Turkey (Serdaroğlu *et al.* 2016; Kasapkara *et al.* 2014; Lonlay *et al.* 2001), New Zealand (Lynn *et al.* 2012), and Spain (Lonlay *et al.* 2001; Meunier *et al.* 2013). The majority of mutations in the *BCS1L* cause encephalopathy, hepatic failure, and proximal tubulopathy. Some mutations cause muscle weakness and optic atrophy (Meunier *et al.* 2013) or Björnstad syndrome (Table 1). Björnstad syndrome is the least severe phenotype, presenting in newborn infants as congenital neurosensory deafness and brittle hair, but compatible with otherwise normal life into adulthood (Hinson *et al.* 2007; Falco *et al.* 2017).

2.5 GRACILE syndrome

A population bottleneck in Finland in the 16^{th} century caused a founder effect in the surviving population and resulted in an accumulation of more than 40 recessively inherited mutations, so-called Finnish disease heritage (Norio 2003), One of these mutations located in *BCS1L* (*c.A232G*, Ser78Gly) causes the GRACILE syndrome. The mutated protein has decreased capacity to incorporate RISP into $CIII_2$ and thereby leads to CIII dysfunction. The lethal phenotype presents typically with severe fetal growth restriction, fulminant lactic acidosis during the first day of life, hepatopathy with cholestasis, proximal tubulopathy with typical aminoaciduria, iron overload with iron accumulation in liver and spleen (Fellman *et al.* 1998). Symptomatic treatments

including a high amount of bicarbonate had only a short-lasting effect. So far more than 40 severe cases with Finnish ancestors have been reported, and the majority of the infants survived less than one month (Fellman *et al.* 1998; Fellman 2002).

Table 1. Human *BCS1L* mutations, the resulting amino acid changes, and clinical phenotypes

Mutation	Amino acid Change	Clinical phenotypes	Reference
Homozygous mutation			
c.148 A>G	T50A	Psychomotor retardation, dysmorphic features, failure to thrive, hypotonia, lactic acidosis, mild sensorineural hearing loss, and hepatic dysfunction	(Blázquez *et al.* 2009)
c.232A>G	S78G	Growth restriction, aminoaciduria, cholestasis, iron overload, lactic acidosis, and early death	(Fellman 1998, 2002, Kotarsky 2010)
c.296C>T	P99L	Acidosis, hepatic failure, and neurologic symptoms, consistent with a Leigh syndrome GRACILE- like a disease	(Kasapkara *et al.* 2014; De Meirleir *et al.* 2003; Serdaroğlu *et al.* 2016)
c.385G>A	G129R	Muscle weakness and optic atrophy.	(Tuppen *et al.* 2010; Al-Owain *et al.* 2013)
c.830G>A	S277N	Neonatal tubulopathy, hepatic failure, and encephalopathy	(de Lonlay *et al.* 2001)
c.901T>A	Y301N	Björnstad syndrome	(Siddiqi *et al.* 2013)
Compound heterozygous mutation			
c.133C>T c.166C>T	R45C R56X	Lactic acidosis, severe failure to thrive, liver dysfunction, renal tubulopathy, iron overload in aggregated macrophages, neurological symptoms, nystagmus, microcephaly, and hypertonia.	(Visapää *et al.* 2002; Lynn *et al.* 2012; Ramos-Arroyo *et al.* 2009)
c.399delA c.306A > T	E133DTer25 G102=	Encephalopathy, lactic academia, muscular hypotonia, psychomotor defect.	(Tegelberg *et al.* 2017)
c.548G>A c.547C>T c.550C>T	R183H, R183C R184C	Encephalopathy, lactic acidosis, psychomotor delay, hypotonia, seizures, failure to thrive, and brittle hair Björnstad syndrome	(Hinson *et al.* 2007)
c.464G>C c.1057G>A	R155P V353M	Leigh syndrome	(Gil-Borlado *et al.* 2009)
c.550C>T c.103G>C	R184C G35R	Encephalopathy, lactic acidosis, psychomotor delay, hypotonia, seizures, failure to thrive, and brittle hair	(Hinson *et al.* 2007)
c.217C >T c.1102T>A	R73C F368I	Encephalopathy, lactic acidosis, psychomotor delay, hypotonia, seizures, failure to thrive, and brittle hair	(Fernandez-Vizarra *et al.* 2007)
c.316G>? c.904C>G c.871C>T c.341G>T c.917G>A	I106Ter Q302E R291Ter R114W R306H	Björnstad syndrome	(Zhang *et al.* 2015) (Siddiqi *et al.* 2013)
c.431G>A c.232A>G	R144Q S78G	Neurological symptoms	(Fellman 2002)
c.980T>C c.166C>T	V327A R565X	Neurological symptoms	(Visapää *et al.* 2002)

2.5.1 The mouse model carrying the GRACILE syndrome mutation

Based on the genotype-phenotype consistency in GRACILE syndrome, Fellman's group set out to develop a mouse model carrying the patient mutation to study disease mechanisms. The homozygotes of this knock-in *Bcs1l*$^{c.A232G}$ mouse model are viable and born healthy, but develop growth restriction with hepatopathy and tubulopathy after weaning (Levéen *et al.* 2011). The mutation decreases the amount of BCS1L in liver mitochondria both at pre- and post-weaning age, (Levéen *et al.* 2011). At two weeks of age (P14), the homozygous liver still has a normal RISP level in CIII and SC (Davoudi *et al.* 2014) and a healthy metabolic profile with slightly decreased AMP (Kotarsky *et al.* 2012). After three weeks of age (P21), homozygous mice rapidly developed growth failure, lactic acidosis, hepatopathy (with glycogen depletion, steatosis, fibrosis), and tubulopathy (Levéen *et al.* 2011). At the deterioration stage, visceral organs such as liver and kidney (Davoudi *et al.* 2014) had low CIII activity and decreased mitochondrial respiration (Levéen *et al.* 2011). The mice typically survived one month, but about 5% of mice in a mixed background to between P70-165 (Levéen *et al.* 2011). In a congenic background (C57BL/6JBomTac) the survival is consistently P35-40 days (Davoudi *et al.* 2016).

2.6 Therapeutic strategies for respiratory chain dysfunction

Therapeutic strategies to improve mitochondrial function include dietary supplementations and pharmacological interventions (Nightingale *et al.* 2016), as well as gene therapy aiming at expressing the wild-type protein (Wallace *et al.* 2010).

As a symptomatic treatment, supplementation with various pharmacological substances including vitamin combinations such as thiamine, riboflavin (Udhayabanu *et al.* 2017), vitamin C, and vitamin E (Parikh *et al.* 2009; Avula *et al.* 2014) have been tested with little effect. In some specific cases, metabolic modifiers such as coenzyme Q10 (ubiquinone) (Neergheen *et al.* 2017), N-acetylcysteine (Viscomi *et al.* 2010), L-carnitine (Mermigkis *et al.* 2013), L-arginine, and citrulline (Koga *et al.* 2005) have been beneficial. L-arginine and citrulline are a suggested therapeutic option for mitochondrial encephalopathy with lactic acidosis (MELAS)-related stroke-like episodes (Koga *et al.* 2005). Dichloroacetate (DCA) is an option to treat lactic acidosis, which is a common problem in mitochondrial disorders. However, DCA can lead to irreversible peripheral neuropathy (El-Hattab *et al.* 2017). Though treatment with these compounds showed some beneficial effects, their efficacy is minimal.

Several studies have tested novel therapeutic strategies in experimental models of various mitochondrial diseases. In *Drosophila* and mouse models, N-acetylcysteine (Wright *et al.* 2015) and

rapamycin (Wang *et al.* 2016) have been beneficial. Peroxisome proliferator-activated receptor γ coactivator 1α (PGC-1α) showed neuroprotective effects by increasing mitochondrial biogenesis and function (Dabrowska *et al.* 2015). Thus, activating PGC-1α is a potential treatment approach for mitochondrial dysfunction due to its role in mitochondrial biogenesis. PGC-1α activation requires either phosphorylation by AMP-dependent kinase (AMPK) or deacetylation by Sirtuin 1 (SIRT1) (Puigserver & Spiegelman 2003). Upregulation of AMPK and *Sirt1* is possible by AICAR and NAD^+ precursors (i.e., nicotinamide riboside, NR) respectively. The administration of AICAR, NR or PARP inhibitors induced mitochondrial biogenesis in myopathy mouse models (Viscomi *et al.* 2011; Cerutti *et al.* 2014; Khan *et al.* 2014). Kennedy *et al.* reported that ketogenic diet (KD) induces the PGC-1α expression via AMP-activated protein kinase (AMPK) signaling (Kennedy *et al.* 2007). KD ameliorated mitochondrial dysfunction and disease progression in pyruvate dehydrogenase deficiency, Med30 mutation, and CI deficiency models (Kim & Rho 2008; Boison 2017; Clanton *et al.* 2017).

Several studies during the past ten years have shown that it is possible to bypass a RC blockage using xenogenes such as NADH reductase (Ndi1) or alternative oxidase (AOX). These proteins are non-proton-pumping enzymes derived from yeast or lower animals. These enzymes have been beneficial in experimental models of RC dysfunction. Ndi1 can bypass a CI defect (Perales-Clemente *et al.* 2008; Sanz *et al.* 2010), and AOX can bypass CIII and CIV defects (Dassa *et al.* 2009; Fernandez-Ayala *et al.* 2009). Both proteins can re-establish the electron flow and decrease the accumulation of reduced ubiquinone and ROS production. Introduction of adeno-associated viruses (AAVs) expressing the wild-type form of the mutated gene is theoretically the most efficient therapy (Di Meo *et al.* 2012; Torres-Torronteras *et al.* 2014) but has technical challenges including poor targeting to the affected organ (Mingozzi & High 2011).

2.7 Alternative oxidases (AOXs)

Alternative oxidases (AOXs) are membrane-associated proteins (Figure 3a) located on the matrix side of IMM. AOX is found in plants (Bahr & Bonner 1973), as well as in some fungi (Veiga *et al.* 2003) and protists (Suzuki *et al.* 2004; Hellemond *et al.* 2007). Furthermore, AOX has also been discovered in 28 lower animal species representing nine different phyla such as *Porifera, Placozoa, Cnidaria, Mollusca, Annelida, Nematoda, Echinodermata, Hemichordata* and *Chordata* (McDonald & Vanlerberghe 2004 and 2006). However, there is no evidence of AOX in vertebrates or arthropods (McDonald *et al.* 2009). AOX transfers electrons from QH_2 to molecular oxygen and releases heat, without coupling to proton translocation. Thus, AOX does not contribute to the proton gradient and ATP production.

AOX functions as a homodimer formed by two monomers bound by an oxidized and covalently linked disulfide bond. AOX has a di-iron carboxylate active site formed by four glutamates (Glu123, 162, 213, and 266) (Figure 3b) and two histidines (His165, 269). Shiba *et al.* reported that a tyrosine residue (Tyr220) plays a role in the catalytic activity (Shiba *et al.* 2013). All these residues are universally conserved (McDonald & Vanlerberghe 2004). In animal phyla, AOX (i.e., *Ciona intestinalis* AOX) lacks the N-terminal regulatory cysteine (Rhoads *et al.* 1998; McDonald *et al.* 2009). Generally, AOX remains inactive until the cytochrome-linked RC complexes (CIII and CIV) become impaired, resulting in an over-reduced quinone pool (accumulation of QH_2) (Vanlerberghe 2013). In plants, accumulation of NADH and pyruvate activate AOX. Their di-sulphide bond reduction by NADH and stabilization by pyruvate result in an active and non-covalently linked AOX homodimer (Vanlerberghe *et al.* 1995). AOX can maintain mitochondrial respiration, decrease ROS by normalizing quinone pool redox status, as well as induce anti-oxidant defenses (Maxwell *et al.* 1999; Amirsadeghi *et al.* 2006; Cvetkovska and Vanlerberghe 2012).

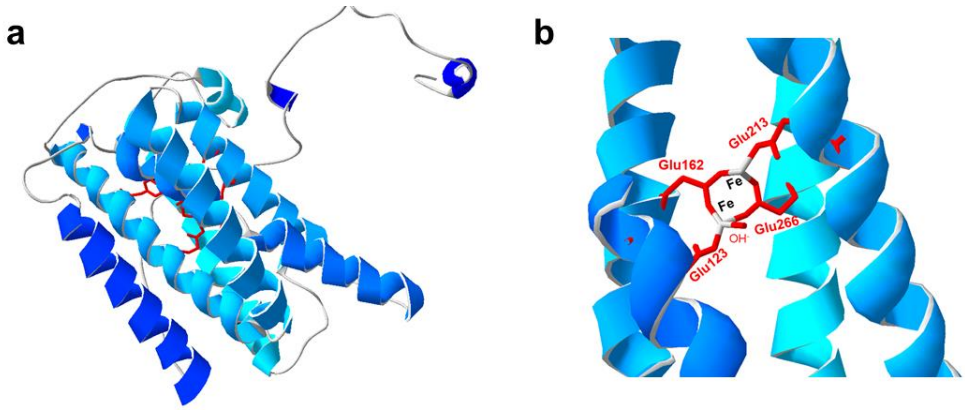

Figure 3. The structure of alternative oxidase (AOX) from *Trypanosoma brucei*. a) Helix bundle of AOX monomer, and b) di-iron carboxylate active site of AOX formed by four glutamate residues. The structure was obtained from the protein data bank (PDB.ID:3VV9).

2.7.1 Experimental models with AOX transgene expression

Ciona intestinalis is an Ascidian (sea squirt) that belongs to the subphylum *Urochordata* or *Tunicata*. *Ciona* expresses AOX in several different cell types during all developmental stages (McDonald & Vanlerberghe 2004). A *CiAOX* transgene was first successfully expressed in human

cells (HEK293T) in 2006 (Hakkaart *et al.* 2006). The cells had a normal growth rate, morphology, respiration, and RC complex functions. Inhibition of respiration using either antimycin A or cyanide showed that AOX rescued respiration and alleviated superoxide overproduction in these cells. This study suggested that the redox status of the ETC regulates the activity of *Ci*AOX in the presence of pyruvate (Hakkaart *et al.* 2006). Other studies of *Ci*AOX expression in COX15 or COX10 (Antonicka *et al.* 2003a and 2003b; Dassa *et al.* 2009) deficient human cells, showed partially rescued respiration, alleviated glucose and pyruvate dependency, and ameliorated growth defect in glucose-restricted condition. Moreover, AOX aided COX15-deficient cells to overcome oxidative-stress-induced apoptosis caused by antimycin or H_2O_2 (Dassa *et al.* 2009).

Whole-body expression of AOX in *Drosophila melanogaster* decreased ROS production under defective cytochrome c pathway (Sanz *et al.* 2010; Kemppainen *et al.* 2014). It also revealed that mitochondrial ROS production in flies does not directly regulate lifespan (Sanz *et al.* 2010). Moreover, ubiquitous or nervous system-specific expression of AOX decreased ROS in the *dj-1β* mutant flies, which is a *Drosophila* model of Parkinson's disease (Kemppainen *et al.* 2014). Another study showed that AOX prevented the loss of dopaminergic neurons in *Drosophila* (Humphrey *et al.* 2012).

A mouse line carrying a single copy of *Ci*AOX in the *Rosa26* locus, which expresses AOX in all tissues, was recently characterized (Szibor *et al.* 2016). AOX expression affected neither RC complexes nor SC formation. AOX was active only under cytochrome-linked complex inhibition by antimycin A or cyanide in these mice. Activated AOX reduced mitochondrial ROS caused by succinate oxidation, and restored upstream respiration. The $Rosa26^{AOX}$ mice showed no phenotypic changes in extensive phenotyping at the German Mouse Clinic (Szibor *et al.* 2016). These studies with *Ci*AOX in various systems such as human cells, fly, and mouse suggest that AOX can function as electron bypasser for cytochrome-linked electron blockade and can ameliorate or prevent tissue pathology.

3 Objectives

The overall objective was to examine the disease mechanism in *Bcs1l* mutant mice and to investigate interventions to ameliorate their disease progression.

Specific Aims

1. To investigate the effect of dietary interventions on disease progression and metabolism in *Bcs1l*$^{p.S78G}$ mice.

2. To examine the effect of AOX-mediated CIII bypass on disease manifestations in *Bcs1l*$^{p.S78G}$ mice.

3. To gain insight into the mechanisms of the tissue-specific manifestations of CIII deficiency.

4 Materials and methods

4.1 Animal strains and husbandry

For the high-carbohydrate study, we used homozygous *Bcs1l*$^{c.A232G}$ (*Bcs1l*$^{p.S78G}$) mutant mice in the C57BL/6JBomTac background (reported as C57BL/6NCrlLtcf in earlier publications) in Lund University (**I**). For the KD and AOX studies, we used the C57BL/6JCrl background in animal facilities at the University of Helsinki (**II**, **III**) after embryo transfer from Lund. The mice were backcrossed for several generations to C57BL/6JCrl before the studies. The mice were housed in open cages at Lund facility and in individually ventilated cages at Helsinki facility. The cages were maintained on 12 h light/dark cycle at 22-23°C. A standard rodent diet (Teklad Global 18% Rodent Diet, Harlan) was used for mice maintenance. Food pellets were provided inside the cage to ensure availability of food to the sick mice.

For the AOX study, we crossed the heterozygous *Bcs1l*$^{p.S78G}$ mutant mice in the C57BL/6JCrl background with AOX transgenic mice in the C57BL/6JOlaHsd background (Szibor *et al.* 2016) to produce *Bcs1l*$^{p.S78G}$ mice carrying the AOX transgene (double heterozygotes). Crossing the double heterozygotes with *Bcs1l*$^{p.S78G}$ heterozygous mice produced *Bcs1l*$^{c.A232G}$ homozygotes expressing AOX (*Bcs1l*$^{p.S78G}$*; Rosa26*^{AOX}, labeled as GROX). The plain homozygotes (*Bcs1l*$^{p.S78G}$) are labeled GRAC, the mice carrying the AOX transgene only as AOX, and wild-type mice as WT (**III**) for this study.

4.2 Genotyping

DNA isolated either from a piece of tail or an ear punch was used for genotyping *Bcs1l* (Levéen *et al.* 2011) and *AOX* transgene (Szibor *et al.* 2016) as described in articles (**I**, **II**,&**III**).

4.3 Dietary interventions

Breeding pairs or litters were randomized to the experimental or control diet. We used a standard rodent diet (Teklad Global 18% Rodent Diet, Harlan) as a control diet. As experimental diets, we used A 60% dextrose diet (TD05256, Harlan) (**I**) and a ketogenic diet (TD.96355, Harlan) (**II**). The experimental diets were introduced into the cages before weaning to familiarize the pups to the diet (**I**&**II**).

4.4 Monitoring deterioration of the *Bcs1l*$^{p.S78G}$ mice

An in-house behavioral scoring method was developed based on common mouse behavioral assessment and the characteristic features of *Bcs1l* mutant mice. It exhibits the sickness of the *Bcs1l*$^{p.S78G}$ mice, which helps to determine the sacrificing point and avoid spontaneous death.

Sickness percentage, relative to the littermate controls, was calculated from the behavioral score and weight loss. The scoring and calculation methods were described in the article **I** and used for all the studies (**I**, **II**, &**III**) in my thesis.

4.5 Blood sampling from living mice

For blood sampling from live mice, the mice were lightly anesthetized with isoflurane (792632 Sigma-Aldrich), and the tail artery vain was punctured with a needle to obtain a blood drop for glucose, lactate and ketone measurements.

4.6 Plasma and tissue collection

The mice sacrification was performed either by cervical dislocation or terminal anesthesia with pentobarbital. Blood was collected into Li-heparin vials (Vacuette 454089, Greiner Bio-One International Gmbh) by cardiac puncture after opening the thoracic cavity. Plasma was isolated and stored as described in (**I**). Organs were snap frozen in liquid nitrogen or fixed in 10% formalin for 24-72 hours, followed by storage in 70% ethanol for histology studies.

4.7 Phenotyping at German Mouse Clinic (GMC)

Mice (n=10 per genotype per sex) were shipped to the GMC at the age of seven weeks and maintained under the GMC housing conditions (www.mouseclinic.de) and according to German laws until sacrification at week 21. The phenotypic screening was performed between ages P56-P112. The experiments conducted at GMC are listed (Table 2), and their protocols are available on the GMC website (www.mouseclinic.de).

4.8 Other experimental methods

The primary assessments performed in Lund and Helsinki are listed below (Table 3). Their detailed protocols are provided in the respective articles.

4.9 Statistics

Details on the statistical methods for each study are reported in respective articles (**I**, **II**, &**III**). For the unpublished data reported in this thesis, one-way ANOVA followed by Tukey's test was performed for group comparisons. Significant differences between the groups in figures are indicated as follows $*p<0.05$; $**p<0.01$; $***p<0.001$. GraphPad Prism 7 software (GraphPad Software Inc, USA) was used to generate the graphs and statistical analysis. Statistical tests used for the data are described in the figure legends.

4.10 Ethical considerations

All the experiments were carried out under the guidelines of the Federation of Laboratory Animal Science Associations (FELASA) with the approval of respective regional animal research ethics committees. The ARRIVE (Animal Research: Reporting of In-Vivo Experiments) recommendations and 3Rs (Replacement, Refinement, and Reduction) regulations were followed. The permission for HCD study was acquired from the animal research ethics committee of Lund region, Sweden (permission M245-11, 19 October 2011), and for KD and AOX gene therapy studies from the ethical committee of the State Provincial Office of Southern Finland (permit numbers ESAVI-2010-07284/Ym-23, and ESAVI/6142/04.10.07/2014). Power and experimental size were calculated separately for each study and details are given in respective articles.

Table 2. General methods used at GMC for phenotyping

GMC Module	Parameter set	Female age range (days)	Male age range (days)	Responsible Researchers
Behavior	Open Field	59-64	52-56	Dr. Sabine M.Hölter
	Acoustic startle and PPI	73-78	66-70	Dr. Lillian Garrett
				Dr. Annemarie Zimprich
				Dr. Wolfgang Wurst
Neurology	SHIRPA	66-71	59-63	Dr. Lore Becker
	Rotarod		66-70	”
Metabolism	Calorimetry TSE	80-85	73-77	Dr. Jan Rozman
Clinical Chemistry	Simplified IPGTT	94-99	87-91	Dr. Birgit Rathkolb
	Clinical chemistry	115-120	108-112	”
	Blood insulin concentration	115-120		”
	Hematology		108-112	”
Dysmorphology	X-Ray	101-106	94-98	Dr. Robert Brommage
				Dr. Helmut Fuchs
				Prof. Dr. Martin Hrabe de Angelis
Nociceptive	Hotplate	101-106	94-98	Dr. Lore Becker
Eyes	Eye size	108-113	94-98	Dr. Oana Veronica Amerie
	Optical coherence tomography	108-113	101-105	
	Scheimpflug analysis	108-113	101-105	Prof. Dr. Jochen Graw
	Virtual drum	108-113	101-105	”

SHIRPA: **S**mithKline Beecham, **H**arwell, **I**mperial College, **R**oyal London Hospital, **p**henotype **a**ssessment; TSE-TSE system; IPGTT-Intra peritoneal glucose tolerance test;

Table 3. The list of experiments performed in our studies.

Experiments	HCD	KD	AOX
Phenotyping			
DEXA			**III**
CLAMS			**III**
Echocardiography			**III**
Blood pressure			**III**
Clinical chemistry			
Plasma			**III**
Urine			**III**
Histology			
Immunohistochemistry			**III**
H&E staining	**I**	**II**	**III**
PAS staining	**I**	**II**	
ORO staining		**II**	**III**
Fibrosis staining		**II**	**III**
Brain immunochemistry			**III**
Lipid peroxidation assay			**III**
Protein analyses			
Western blotting			**III**
Blue native PAGE	**I**		**III**
Mitochondrial assessment			
Electron microscopy		**II**	**III**
CIII activity			**III**
Respirometry	**I**		**III**
Mitochondrial H_2O_2 emission			**III**
Metabolomics			
Plasma metabolomics	**I**	**II**	
Tissue metabolomics			**III**
Transcriptomics			**III**

HCD-high carbohydrate diet; KD-ketogenic diet; AOX-alternative oxidase; DEXA- dual-energy x-ray absorptiometry; CLAMS- CLAMS Comprehensive Lab Animal Monitoring System; H&E-hematoxylin and eosin; PAS-periodic acid–Schiff; Oro-Oil Red O.

5 Results

5.1 Plasma metabolome in *Bcs1l*$^{p.S78G}$ mice with and without dextrose supplementation (I)

Earlier studies of *Bcs1l*$^{p.S78G}$ mice have focused on the metabolism and CIII assembly and function in liver tissue (Levéen *et al.* 2011; Kotarsky *et al.* 2012; Davoudi *et al.* 2014). In this study, we assessed the metabolite changes in plasma, through which the metabolic crosstalk between organs occurs. Plasma metabolomics in *Bcs1l*$^{p.S78G}$ mice revealed increased protein catabolism, defective beta-oxidation, and metabolic response to oxidative stress. Our interpretations suggest that the glucose-alanine cycle and protein catabolism were high due to the hypoglycemic condition in *Bcs1l*$^{p.S78G}$ mice. Furthermore, we found changes in kidney disease-associated plasma metabolites such as phenylalanine, ornithine, and asymmetric-dimethyl arginine. The high-carbohydrate (60% dextrose) diet (HCD) on *Bcs1l*$^{p.S78G}$ mice did not relieve the hypoglycemia, loss of hepatic glycogen, micro-vesicular fat accumulation, or decreased mitochondrial respiration. Unexpectedly, the HCD slightly decreased survival, despite partially normalizing some plasma metabolites related to amino acid metabolism, urea cycle, and neurotransmitter intermediates.

5.2 Effect of ketogenic diet (KD) in adult *Bcs1l*$^{p.S78G}$ mice (II and unpublished)

For the KD feeding study, we used the *Bcs1l*$^{p.S78G}$ mutants of C57BL/6JCrl background, in which the homozygotes survive up to 200 days, probably because they escape the lethal hypoglycemia in the juvenile stage. Aiming to bypass glucose metabolism, we fed KD to two mouse groups from weaning on. We sacrificed the mice for end-point analyses at P45 (young age) or P95 (adult age) and investigated the effect of the diet on hepatopathy (**II**). The data on adult mice (over P60) are summarized as follows. *Bcs1l*$^{p.S78G}$ mice at P95 had lower blood glucose and increased lactate per glucose ratio. The liver enzymes alanine transferase and alkaline phosphatase were high in plasma (**II**, Table 1). Hepatic histology at P95 revealed prominent fibrosis, increased fat, decreased glycogen, and increased apoptotic cells (**II**, Fig 2, Supplementary Fig.2). We found changes in plasma metabolites related to protein catabolism, urea cycle, bile acids, and acylcarnitines (**II**, SupFig10B,11B.). Hepatic mitochondria of *Bcs1l*$^{p.S78G}$ mice were significantly smaller in size and had a low number of thickened cristae (**II**, Fig3). Our findings confirmed the persistence of liver dysfunction in adult *Bcs1l*$^{p.S78G}$ mice. However, the hepatopathy was not severe enough to be the cause for the deterioration.

KD did not affect the growth of *Bcs1l*$^{p.S78G}$ mice, but robustly induced ketosis. Their liver histopathology at P95 showed amelioration of ductular reactions, portal inflammation, fibrosis, and apoptosis. It indicated that the effect of KD on hepatopathy was persistent also at adult age

(**II**, Fig1A-D). Moreover, KD rescued mitochondrial morphology (**II**, Fig3), and partially rescued alkaline phosphatase and urea cycle intermediates (arginine, and ornithine) in plasma. Furthermore, decreased carnitine and short-chain acylcarnitine levels in plasma of KD-fed *Bcs1l*$^{p.S78G}$ mice indicated altered fatty-acid metabolism (**II**, SupFig10B,11B.). However, KD-fed *Bcs1l*$^{p.S78G}$ mice deteriorated earlier than the mice on standard/control diet (CD).

We investigated the KD effect on survival of *Bcs1l*$^{p.S78G}$ mice using another mouse panel. One group of mutant mice (n=4/genotype) were fed on KD until deterioration, and for another group (n=3/genotype) we replaced KD at P50 with the CD. On CD, the mutant mice survived to median 163 days, whereas those on KD started to deteriorate earlier with a median survival of 102 days (Figure **4**a). The sickness curves, generated based on the combination of sickness score and weight loss, suggested intolerance of *Bcs1l*$^{p.S78G}$ mice to KD over time (Figure 4b). Diet change did not affect blood glucose but had a significant impact on blood ketone body and lactate per glucose ratio (Figure 4c-e).

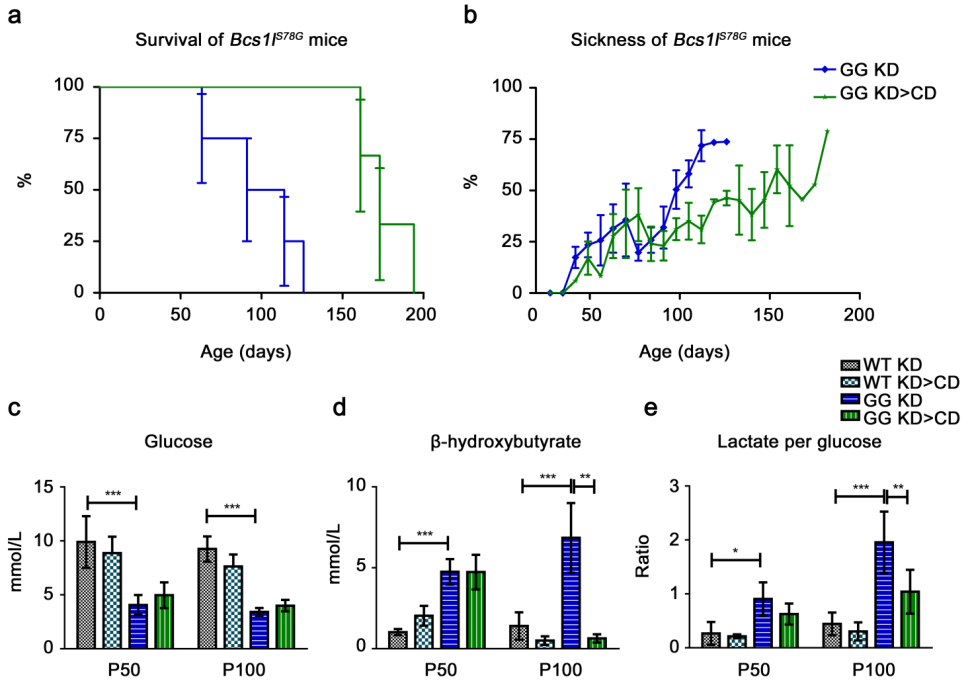

Figure 4. Sickness score and survival of *Bcs1l*$^{p.S78G}$ mice on KD. a) Survival (p=0.0177, Log-rank, Mantel-Cox Test), b) sickness as determined from behavioral scoring and weight loss, c) blood glucose, d) β-hydroxybutyrate, and e) lactate per glucose ratio. KD>CD indicates a shift of KD to CD after P50. Bar graphs plotted with mean±SD. One way ANOVA followed by Tukey's test for group comparisons. *p<0.05; **p<0.01; ***p<0.001.

5.3 *Bcs1l*$^{p.S78G}$ mice expressing AOX (GROX mice) (III and unpublished)

5.3.1 AOX extended the survival of *Bcs1l*$^{p.S78G}$ mice with little effect on growth, whole-body metabolism and behavior (III and unpublished)

To assess the effect of AOX-mediated CIII bypass on disease progression, we bred wild-type and *Bcs1l* mutant mice with and without AOX transgene (labeled in figures, wild-type as WT, *AOX*$^{+/-}$ as AOX, *Bcs1l*$^{p.S78G}$ as GRAC, and *Bcs1l*$^{p.S78G}$*; AOX*$^{+/-}$ as GROX). We found that AOX expression drastically increased the median survival of the *Bcs1l*$^{p.S78G}$ mice (in GROX mice) from P210 to P590 days (**III**, Fig1B).

A striking early phenotype of GRACILE syndrome patients and *Bcs1l*$^{p.S78G}$ mice is their growth restriction (Fellman *et al.* 1998; Visapää *et al.* 2002; Levéen *et al.* 2011). GMC performed extensive phenotyping of young *Bcs1l*$^{p.S78G}$ mice (P56-120) and showed decreased body weight, lean weight, fat mass, and bone mineral density in the GRAC mice. Interestingly, AOX expression did not cause a drastic improvement in body weight (**III**, Fig1D-G). Behavioral phenotyping (between P52-64) showed that the *Bcs1l*$^{p.S78G}$ mice were less active in the open field test (Figure **5**a-c). Decreased respiratory exchange rate (in females) and heat production (III, Fig1H, I) suggest decreased whole-body energy metabolism. AOX expression in *Bcs1l*$^{p.S78G}$ mice (GROX) had no effect on activity or energy metabolism.

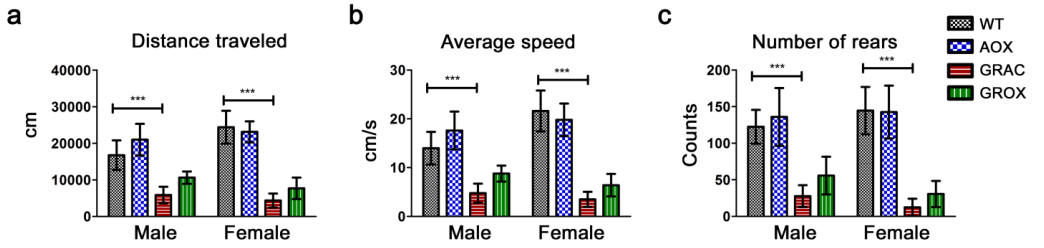

Figure 5. Motor activity in GRAC mice. (a) Total distance traveled by mice in the open field, (b) average speed of the mice passing through the center, (c) rearing activity. Bar graphs plotted with mean±SD. One-way ANOVA followed by Tukey's test for group comparisons. *p<0.05; **p<0.01; ***p<0.001.

Hematological analysis of GRAC mice revealed smaller platelet volume and less red blood cell distribution width (RDW)(Table 4). Glucose tolerance test showed no change of tolerance (after 30 or last 90 min of glucose injection), despite low basal glucose level (Table 5 and Table 6). Additionally, blood chemistry revealed only marginal alterations in blood electrolytes such as calcium, sodium, and slightly increased iron concentration, but significant changes in the liver

enzymes such as alkaline phosphatase (ALP), aspartate aminotransferase (ASAT), alanine aminotransferase (ALAT), and lactate dehydrogenase (LDH) (Table 5 and Table 6). AOX expression (in GROX) did not alter hematology or blood composition. However, it did decrease the elevated liver enzymes in females at P108-120.

Table 4. The hematology of male mice (P101 - P121).

	WT	AOX	GRAC	GROX
Hematocrit	51.9 ± 2.1	51.8 ± 1.7	49.3 ± 2.5	50.5 ± 1.4
Hemoglobin	16.6 ± 0.6	16.6 ± 0.8	16.0 ± 0.9	16.3 ± 0.6
MCHCont	15.7 ± 0.5	15.6 ± 0.4	15.7 ± 0.4	16.1 ± 0.4
MCHC	32.0 ± 1.0	32.1 ± 0.8	32.5 ± 0.8	32.3 ± 0.8
MCV	49.1 ± 1.5	48.4 ± 1.0	48.3 ± 0.7	50.1 ± 0.7
Mean platelets volume	6.3 ± 0.1	6.2 ± 0.1	5.9 ± 0.1*	6.1 ± 0.2
PDW	5.5 ± 0.1	5.4 ± 0.2	5.1 ± 0.1	5.3 ± 0.2
Platelet large cell ratio	2.7 ± 0.5	2.3 ± 0.6	1.5 ± 0.3	2.0 ± 0.6
Platelet count	981.6 ± 164.6	1072.7 ± 122.3***	1049.6 ± 82.1***	1064.1 ± 70.3
Red blood cell count	10.6 ± 0.4	10.7 ± 0.3	10.2 ± 0.5	10.1 ± 0.3
RDW	14.3 ± 0.3	14.2 ± 0.5	12.7 ± 0.4*	12.9 ± 0.3
White blood cell count	10.0 ± 2.2	10.7 ± 2.6	11.1 ± 1.5	12.1 ± 3.0

MCHCont: Calculated mean corpuscular hemoglobin content of erythrocytes; **MCHC**: Calculated mean corpuscular hemoglobin concentration of erythrocytes; **MCV**: Mean corpuscular volume; **PDW**: Calculated distribution width of platelets; **RDW**: Red cell distribution width (coefficient of variation). Data represented as mean±SD. One-way ANOVA followed by Tukey's test for group comparisons. *, $p<0.05$; **, $p<0.01$; ***, $p<0.001$.

Table 5. Blood chemistry in females (P115-P120).

		Females			
		WT	AOX	GRAC	GROX
IPGTT					
Glucose (T=0)	mmol/l	9.3 ± 2.3	8.9 ± 1.3	4.2 ± 1.2*	5.4 ± 0.6
AUC 30	mmol/l/min	495.5 ± 74.8	477.3 ± 45.6	292.2 ± 74.6*	337.0 ± 71.2
AUC 90	mmol/l/min	969.4 ± 153.7	837.3 ± 313.6	576.8 ± 310.0	725.0 ± 138.1
Electrolytes					
Calcium	mmol/l	2.4 ± 0.1	2.4 ± 0.1	2.7 ± 0.1*	2.6 ± 0.1
Chloride	mmol/l	115.7 ± 2.3	114.2 ± 1.4	117.0 ± 1.6	115.1 ± 4.4
Potassium	mmol/l	4.1 ± 0.3	4.1 ± 0.4	3.9 ± 0.3	4.0 ± 0.3
Sodium	mmol/l	152.1 ± 1.8	151.4 ± 1.4	158.4 ± 1.7*	154.7 ± 4.6
Inorganic phosphate	mmol/l	1.6 ± 0.4	1.5 ± 0.2	2.1 ± 0.4	2.3 ± 0.4
Enzymes					
Alpha-amylase	U/l	567.3 ± 24.3	614.8 ± 47.7	590.9 ± 83.0	702.4 ± 306.6$^{\sharp\sharp}$
Alkaline phosphatase	U/l	136.2 ± 6.2	142.7 ± 15.2	378.7 ± 53.7***	296.2 ± 51.7†
Aspartate aminotransferase	U/l	46.6 ± 6.6	52.7 ± 12.0	621.7 ± 323.0***	339.2 ± 110.5$^{\sharp\sharp}$
Alanine aminotransferase	U/l	37.9 ± 25.6	33.8 ± 13.2	325.8 ± 139.7***	182.2 ± 58.2$^{\sharp\sharp}$
Lactate dehydrogenase	U/l	206.8 ± 67.7	235.5 ± 48.6	536.7 ± 145.5***	403.6 ± 90.0$^{\sharp\sharp}$
Other contents					
Albumin	g/l	29.1 ± 1.2	28.9 ± 1.2	29.0 ± 2.0	26.7 ± 1.7
Cholesterol	mmol/l	2.2 ± 0.2	2.0 ± 0.4	2.0 ± 0.2	1.7 ± 0.2
Creatinine	µmol/l	11.1 ± 2.0	10.5 ± 1.6	11.0 ± 0.7	11.2 ± 2.1
Total protein	g/l	52.7 ± 2.0	52.5 ± 1.8	52.9 ± 2.6	48.8 ± 2.6
Triglyceride	mmol/l	1.0 ± 0.4	1.1 ± 0.2	0.8 ± 0.3	0.9 ± 0.2
Urea	mmol/l	10.9 ± 1.1	12.4 ± 2.1	11.7 ± 1.4	11.2 ± 1.2
Iron	µmol/l	24.7 ± 4.5	29.2 ± 3.1	36.5 ± 6.7*	33.0 ± 4.4
Unsaturated iron binding capacity	µmol/l	34.2 ± 4.0	26.8 ± 5.5	38.0 ± 10.7	32.4 ± 4.9

Data represented as Mean±SD. One-way ANOVA followed by Tukey's test for group comparisons."*" indicates a comparison between WT and GRAC mice, and "♯" indicates a comparison between GRAC and GROX mice. */♯, $p<0.05$; **/♯♯, $p<0.01$; ***/♯♯♯, $p<0.001$.

Table 6. Blood chemistry in males (P108-P112).

		Males											
		WT			AOX			GRAC			GROX		
IPGTT													
Glucose (T=0)	mmol/l	10.4	±	1.9	9.8	±	1.4	5.0	±	0.5***	5.5	±	0.8
AUC 30	mmol/l/min	531.0	±	117.0	515.6	±	57.1	326.8	±	109.1	321.0	±	114.7
AUC 90	mmol/l/min	1050.6	±	309.4	969.4	±	222.9	650.6	±	189.3	670.9	±	222.5
Electrolytes													
Calcium	mmol/l	2.5	±	0.1	2.4	±	0.1	2.7	±	0.1*	2.6	±	0.1
Chloride	mmol/l	108.7	±	2.4	108.0	±	3.4	113.4	±	2.2	111.5	±	2.4
Potassium	mmol/l	4.1	±	0.4	4.0	±	0.4	3.6	±	0.4	3.7	±	0.3
Sodium	mmol/l	150.2	±	2.2	149.0	±	3.8	152.5	±	2.8	151.0	±	2.6
Inorganic phosphate	mmol/l	1.6	±	0.3	1.5	±	0.3	1.8	±	0.3	1.7	±	0.4
Enzymes													
Alpha-amylase	U/l	732.5	±	57.2	718.0	±	27.8	758.8	±	101.3	717.4	±	138.7
Alkaline phosphatase	U/l	105.3	±	8.5	95.3	±	13.3	304.9	±	24.1***	278.1	±	28.3
Aspartate aminotransferase	U/l	56.5	±	11.6	55.3	±	13.1	691.5	±	131.5***	629.7	±	111.7ǂǂ
Alanine aminotransferase	U/l	37.2	±	19.9	40.6	±	11.6	358.7	±	58.8***	318.3	±	49.6
Lactate dehydrogenase	U/l	187.4	±	46.7	189.2	±	50.1	514.0	±	121.0***	473.1	±	74.0
Other contents													
Albumin	g/l	28.5	±	1.4	27.3	±	2.0	27.0	±	0.9	27.7	±	1.1
Cholesterol	mmol/l	2.6	±	0.4	2.5	±	0.3	1.9	±	0.3	2.2	±	0.2
Creatinine	µmol/l	10.1	±	2.0	10.2	±	2.3	13.1	±	3.0	12.1	±	2.4
Total protein	g/l	54.4	±	2.5	53.8	±	2.5	50.8	±	1.7	51.9	±	1.8
Triglyceride	mmol/l	1.9	±	0.5	1.7	±	0.3	1.1	±	0.4	1.3	±	0.5
Urea	mmol/l	12.7	±	1.7	12.5	±	1.4	10.7	±	1.3	9.7	±	1.7
Iron	µmol/l	20.5	±	2.7	20.7	±	1.3	29.1	±	4.2*	28.7	±	2.8
Unsaturated iron binding capacity	µmol/l	38.4	±	4.3	36.5	±	1.6	42.1	±	6.0	36.9	±	3.4

Data represented as Mean±SD. One-way ANOVA followed by Tukey's test for group comparisons."*" indicates a comparison between WT and GRAC mice, and "ǂ" indicates a comparison between GRAC and GROX mice. */ǂ, $p<0.05$; **/ǂǂ, $p<0.01$; ***/ǂǂǂ, $p<0.001$.

5.3.2 AOX preserved CIII activity and prevented late-onset cardiomyopathy (III)

We found that the cause of death of *Bcs1l*$^{p.S78G}$ mice at P200 was most likely a dilated cardiomyopathy. Echocardiography revealed that the cardiac function began to decline after P150 (**III**, FigEV1). Histopathology of *Bcs1l*$^{p.S78G}$ heart at end stage (P200) showed increased fibrosis and oxidative stress (4-hydroxynonenal staining) (**III**, Fig2C-D, and 8E-F). Moreover, heart mitochondria were morphologically abnormal, with smaller size and fewer and thicker cristae (**III**, Fig3B-F).

We sacrificed another mouse group at P150 (at the pre-symptomatic age to cardiomyopathy) to analyze the early transcriptional and metabolite alterations, and to assess mitochondrial function (**III**). We found that heart mitochondria in *Bcs1l*$^{p.S78G}$ mice (GRAC) had significantly lower CIII activity (approx. 34% of WT) and respiration (approx. 17% of WT) (**III**, Fig6). Moreover, transcriptomics analysis revealed changes in energy and nitric oxide metabolism (**III**, Fig5, FigS2, and Fig8A). Remarkably, AOX expression in *Bcs1l*$^{p.S78G}$ mice (GROX) partially rescued cardiac mitochondrial CIII activity (approx. to 50% of WT), fully normalized the respiration (100% of WT), and, surprisingly, increased the amount of RISP in CIII dimers (**III**, Fig6). Furthermore, AOX expression preserved mitochondrial morphology and tissue histology. We found that AOX expression in the *Bcs1l*$^{p.S78G}$ heart normalized the transcriptional changes related to beta-oxidation, amino-acid metabolism, TCA cycle, NO metabolism, and sarcoplasmic-reticulum Ca^{2+} ion channels to WT level. These changes likely contributed to the prevention of lethal cardiomyopathy.

5.3.3 AOX prevented renal tubular atrophy but not hepatopathy (III)

Although *Bcs1l*$^{p.S78G}$ mice (GRAC) survived until P200, their liver fibrosis did not progress to cirrhosis. In contrast, the progressive degeneration in proximal tubules of the kidneys resulted in severe renal atrophy (**III**, Fig2A-B) and affected urine filtration parameters (**III**, FigS1). In both the liver and kidney of *Bcs1l*$^{p.S78G}$ mice, we found a defect in CIII activity and alteration in mitochondrial morphology (**III**). Transcriptomic analysis at post-symptomatic age (P150) showed altered cell proliferation, fibrosis, and energy metabolism. Interestingly, we found increased glutathione metabolism only in the liver (**III**, Fig.5). AOX expression did not affect the progressing hepatopathy at P200. In contrast, AOX expression rescued kidney mitochondrial morphology; decreased proximal tubular cell apoptosis and permanently prevented renal tubular atrophy (**III**).

5.3.4 Effect of AOX on the central and sensory nervous systems (III and unpublished)

The brain of *Bcs1l*$^{p.S78G}$ mice (GRAC) showed no signs of severe neurodegeneration but did exhibit a mild increase in astrogliosis in the barrel field of the primary somatosensory cortex (S1BF), as

reported earlier (Tegelberg *et al.* 2017). AOX expression in *Bcs1l*$^{p.S78G}$ mice robustly delayed the focal astrogliosis (**III**, Fig3A).

Detailed phenotyping at GMC revealed that *Bcs1l*$^{p.S78G}$ mice had no changes in locomotor activity or latency on Rotarod drum. These data suggest no defect in neuromuscular function (Figure 6a,b). However, decreased prepulse inhibition suggested a defect in acoustic startle reactivity and in hearing sensitivity (Figure 6c). Furthermore, the retardation of *Bcs1l*$^{p.S78G}$ males (GRAC) for second heat stimulation in hot plate assay indicated a defect in the neurosensory system (Figure 6d).

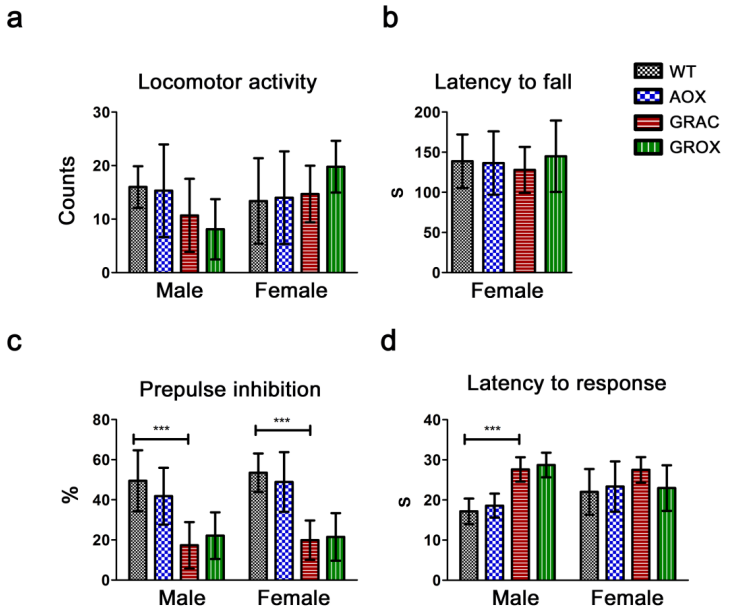

Figure 6. Neuronal responses in GRAC and GROX mice. (a) Locomotor activity, (b) latency to fall from Rotarod drum, (c) response to prepulse inhibition, and (d) latency to response for second heat stimulation on hot plate assay. Bar graphs plotted with mean±SD. One-way ANOVA followed by Tukey's test for group comparisons. *p<0.05; **p<0.01; ***p<0.001.

Laser interference biometry on *Bcs1l*$^{p.S78G}$ mice (GRAC) indicated reduced axial eye lengths (distance between cornea and retina) (Figure 7a), reduced lens thickness (Figure 7b) and small anterior chamber (Figure 7c) which correlated with small body size. Optical coherence tomography (OCT) investigation showed that the posterior part of the eye was healthy with normally developed fundus and blood vessels (Figure 7d, e), but a mild change in corneal and retinal thicknesses (Figure 7f-i). However, the vision test revealed that *Bcs1l*$^{p.S78G}$ mice (GRAC) had weaker responses than wild-type to the moving stripe pattern of the virtual drum (Figure 7j). AOX expression on

Bcs1l$^{p.S78G}$ mice improved the eye-axial length and alleviated the lens thickness abnormality (Figure 7a, b). Additionally, AOX expression induced a mild amelioration in vision responses to the moving stripe pattern of the virtual drum in males (Figure 7j).

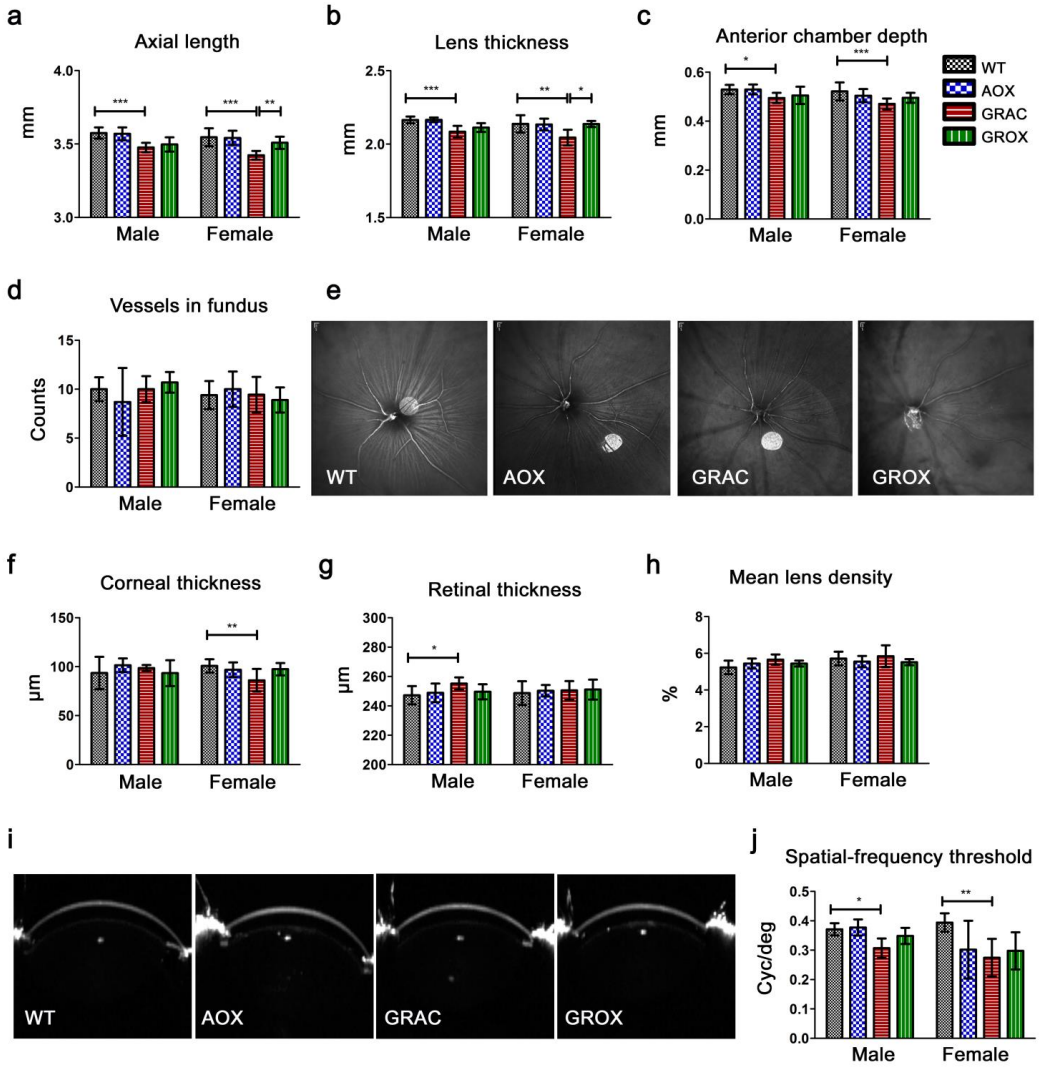

Figure 7. Assessment of vision in GRAC and GROX mice. (a-i) Optical coherence tomography measurements of (a) axial length, (b) lens thickness, (c) anterior chamber depth, (d) number of vessels in fundus, (e) image of posterior part of the eye, thickness of (f) cornea and (g) retina, (h) mean density of the left eye's lens and (i) representative image of lens, and (j) visual response to the moving stripe pattern of the virtual drum. Bar graphs plotted with mean±SD. One-way ANOVA followed by Tukey's test for group comparisons. *p<0.05; **p<0.01; ***p<0.001

5.3.5 Subtle effect of AOX on the cardiac transcriptome in wild-type mice (III and unpublished)

A previous published (Szibor *et al.* 2016) characterization of the AOX transgenic mice reported no overt phenotypic changes. We confirmed that AOX expression in WT mice (pure AOX mice) caused no behavioral or whole body metabolic effects. The AOX mice were also histologically identical to WT controls. However, we found slight but significant differences (p<0.05, |FC|<1.5) in the heart transcriptome of AOX mice with 767 altered genes or transcripts, compared to wild-type mice. Most of the genes are annotated (525 genes) and some are uncharacterized genes (242 are without name and function). Moreover, the vast majority of these annotated genes had no available data on Gene-Ontology enrichment analysis. Interestingly, we found 23 genes associated with mitochondrial functions (Figure 8) such as the TCA cycle or respiration, transmembrane transportation, DNA repair mechanism, and mitochondrial morphology/migration.

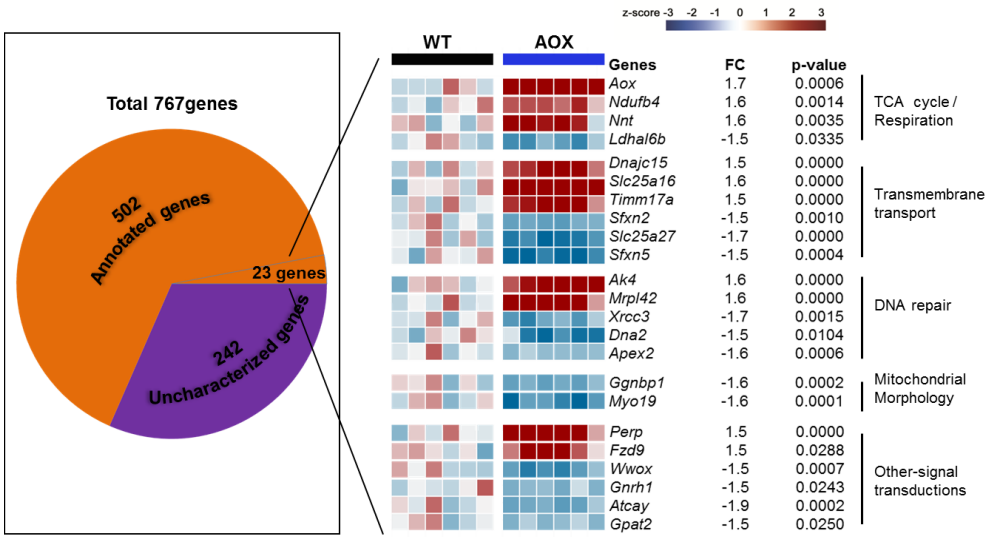

Figure 8. The effect of AOX on heart transcriptome in wild-type mice at P150.

6 Discussion

6.1 Novel manifestations in *Bcs1l*$^{p.S78G}$ mice

During this project, we found in the *Bcs1l*$^{p.S78G}$ mice (in the C57BL/6JCrl background) several novel phenotypes, which have neither been reported in GRACILE patients nor in the earlier mouse studies using another genetic background. The GRACILE syndrome patients present with early hepatopathy and kidney tubulopathy, but no apparent cardiac abnormality during their short lifespan (Fellman *et al.* 1998; Visapää *et al.* 2002). Early lethality in infancy likely explains the lack of the later-onset phenotypes such as encephalopathy, hearing loss, defective visual senses, and cardiomyopathy. However, patients with other *BCS1L* gene mutations can present with encephalopathy (Lonlay *et al.* 2001; Moran *et al.* 2010; Fernandez-Vizarra *et al.* 2007; Tegelberg *et al.* 2017). Björnstad syndrome, also the result of other mutations in *BCS1L*, manifests with sensorineural hearing loss and twisted hair (Hinson *et al.* 2007; Falco *et al.* 2017). Also, a patient with homozygous *BCS1L*$^{p.T70P}$ mutation developed hearing loss (Blázquez *et al.* 2009). Adult patients with the homozygous *BCS1L*$^{p.G129R}$ mutation presented with visual problems and bilateral optic atrophy (Tuppen *et al.* 2010). Thus, it seems that *Bcs1l*$^{p.S78G}$ mice in the C57BL/6JCrl background develop most of the phenotypes reported in patients with *BCS1L* mutations, but also in patients with *MT-CYB* mutations (cardiomyopathy) (Hagen *et al.* 2013).

In homozygotes of the C57BL/6JCrl background at P150, we found that CIII activity was less than 50% of the WT in all affected tissues: heart (34%), kidney (45%), and liver (34%). Moreover, Levéen *et al*. also reported progressive CIII dysfunction in several tissues of *Bcs1l*$^{p.S78G}$ mice. The liver had 50% CIII activity of the WT at disease onset and linear decrease to as low as 20% at end-stage disease (P30). At P30, the cardiac CIII activity in *Bcs1l*$^{p.S78G}$ mice was about 50% of normal with no signs of cardiomyopathy, but kidney CIII activity was 40%, and the mice manifested tubulopathy (Levéen *et al.* 2011). Therefore, our findings related to CIII activity are in line with the notion that the onset of manifestations requires decreased CIII activity to below 50%.

6.2 Dietary interventions

Hypoglycemia is a significant metabolic manifestation of the GRACILE syndrome. *Bcs1l*$^{p.S78G}$ mice in the C57BL/6JBomTac background (**I**) deteriorate at an early age due to the starvation-like conditions and severe hypoglycemia (Levéen *et al.* 2011). Providing high carbohydrate (60% dextrose) diet (HCD) did not improve the glycemic condition. Our results support the conclusion from a previous study (Du *et al.* 2010) that glucose is a metabolically challenging substrate when OXPHOS is defective. Increased dietary glucose partially normalized plasma metabolites related to

amino acids metabolism and the urea cycle. However, this was insufficient to improve the health of the mice. Despite the minor effect of the high-dextrose diet, the plasma metabolomics provided novel insight into the metabolic disease of the *Bcs1l*$^{p.S78G}$ mice.

Ketogenic diet may stimulate fatty acid oxidation and thereby partially relieve dependence on glucose oxidation and PPAR pathway (Kang *et al.* 2007). Our study (II) showed that KD ameliorated hepatopathy and improved mitochondrial structure and function in hepatocytes. Other studies have shown the beneficial effects of KD in patients with epilepsy (Kang *et al.* 2007) and mouse models of pyruvate dehydrogenase deficiency (Sofou *et al.* 2017) and mitochondrial myopathy (Ahola-Erkkilä *et al.* 2010). However, the decreased survival of *Bcs1l*$^{p.S78G}$ mice on KD indicated that the CIII deficiency also caused intolerance to a fat-based diet. As we did not assess the effect of KD on other organs, we cannot address the exact cause of premature death. The short-term KD feeding (P20 to P50) did not decrease the life-span of mutant mice (Figure **4**). Increased blood lactate per glucose ratio at adult age and reduced survival upon long-term KD feeding indicated adverse effect. Our study suggested that KD may have a therapeutic effect on hepatopathy. However, it may cause an adverse effect that prevents its use in patients.

6.3 Transgenic AOX-mediated CIII bypass

AOX expression dramatically extended the survival of *Bcs1l*$^{p.S78G}$ mice (GROX) and was beneficial mainly for the heart and partially for the kidney. AOX expression rescued mitochondrial structure and tissue histology only in heart and kidney tubular cells, suggesting that AOX functioned most prominently in high energy-demanding cells. In cardiomyocytes, decreased nitric oxide metabolism and improved gene expression of sarcoplasmic reticulum (SR) Ca^{2+} channels seem to be the essential pathways associated with the cardiac functional rescue. In the *Bcs1l*$^{p.S78G}$ (GRAC) heart, transcriptomic alterations in NOS1 and NOS3 suggested the possibility for higher reactive nitrogen species (RNS). Other studies have reported the involvement of NOS1 and NOS3 in mitochondrial stress in dilated cardiomyopathy (Crespo *et al.* 2008; Matsa *et al.* 2013).

Moreover, acute or long-term regulation of both ROS and RNS play an essential role in controlling Ca^{2+} flux in chronic heart failure (Searles 2002). The cardiac contraction occurs by Ca^{2+} release and uptake in the sarcoplasmic reticulum (SR) through channels such as ryanodine receptor (RyR) (Ogawa 1994) and SR Ca^{2+}-ATPase (SERCA/ i.e., ATPA2A)-phospholamban (PLN) complex (Frank *et al.* 2003) respectively. A significant decrease in *Ryr2*, *Atp2a2*, and *Pln* genes in the *Bcs1l*$^{p.S78G}$ (GRAC) heart may have caused a defect in the SR-Ca^{2+} release and uptake mechanism.

Several studies have reported SR Ca^{2+}-ATPase reduction and myocardial Ca^{2+} handling in dilated cardiomyopathy (Gupta *et al.* 1997; Gregory *et al.* 2006; Li *et al.* 2012). However, it is unclear whether increased NOS expression in the *Bcs1l*$^{p.S78G}$ (GRAC) heart was a cause or an effect in relation to the altered SR Ca^{2+} channels expression. Further examination of NO metabolism and signaling in the mutant mice may elucidate this.

Royo *et al*. demonstrated in plants that NO and AOX function are linked (Royo *et al.* 2015). AOX-mediated respiration in plants (Millar & Day 1996) and in *Trypanosoma* (Chaudhuri *et al.* 2006) was tolerant to NO stress. Some studies have reported that NO regulates AOX activation, which functions as an antioxidant and anti-nitrosative in plants to protect from viral infection (Gupta *et al.* 2012). Thus, the AOX-mediated rescue of NO metabolism in *Bcs1l*$^{p.S78G}$ heart raises the intriguing possibility that an association between AOX and NO exists in these mice as well.

AOX expression in the *Bcs1l*$^{p.S78G}$ (GROX) kidney rescued tubular cell mitochondrial morphology without normalizing the CI and CII linked respiration in the presence of ADP (state III). Moreover, the transcriptomic analysis in the kidney revealed upregulation of cell cycle pathways that indicate regeneration or induced cell proliferation. A recent report on the effect of AOX expression on muscle-specific COX15 knockout mice also showed that AOX did not normalize mitochondrial state III respiration. Instead, AOX had an adverse effect on the myopathy phenotype by reducing ROS production and impairing regenerative capacity (Dogan *et al.* 2018). In contrast, we found that AOX expression in the kidney of *Bcs1l*$^{p.S78G}$ mice (GROX) significantly decreased mitochondrial stress (implicated by the rescued mitochondrial structure) and apoptosis but did not affect the regeneration or proliferation of renal tubular cells.

7. Conclusions

The studies included in this thesis have further elucidated disease mechanisms and provide novel insight into possible treatment strategies for CIII deficiency. Mitochondrial disorders present with tissue-specific manifestations, but also with unexpected subtle symptoms. By comparing the standardized phenotyping, histological findings, metabolism, transcriptome and mitochondrial function in the tissues of *Bcs1l* mutant mice, we achieved a better understanding of GRACILE syndrome pathogenesis. Our main conclusions are: 1) $Bcs1l^{p.S78G}$ mice in C57BL/6JCrl background survive to P200 and develop novel late-onset phenotypes including kidney atrophy and dilated cardiomyopathy. 2) Dietary interventions have a limited effect on the severe visceral manifestations of $Bcs1l^{p.S78G}$ mice. 3) AOX-mediated CIII bypass efficiently prevents or alleviates manifestations of CIII deficiency. 4) AOX was mainly beneficial in tissues/cells with high ATP demand, such as the heart and proximal tubular cells.

8 Future prospects

Recent whole-genome sequencing of the short-lived *Bcs1l*$^{p.S78G}$ mice, (C57BL/6JBomTac colony), revealed a spontaneous variant in mtDNA. The variant emerged more than ten years ago in the in-house C57BL/6JBomTac colony. We have now verified that the combination of this mtDNA variant and the *Bcs1l*$^{p.S78G}$ mutation resulted in short survival (approx.P35-40) (Purhonen *et al*. under revision). Further characterization regarding the effects of this particular mtDNA variant alone and in combination with the *Bcs1l*$^{p.S78G}$ mutation in the C57BL/6JCrl background is ongoing.

An interesting mechanistic finding from the AOX study was that AOX-mediated respiration might be tolerant of nitric oxide (NO) stress. NO is associated with heart failure and neuronal degeneration. Further examination of the AOX effect on NO stress might clarify the rescue mechanisms and thereby increase knowledge about the possible use of AOX in other mitochondrial diseases. However, transgenic AOX expression is not possible in patients nowadays, But further studies to develop viral delivery of transgene are ongoing.

Drosophila is widely used for genetic studies also with mitochondrial disorders (Sardiello *et al.* 2003; Jacobs *et al.* 2004; Tripoli *et al.* 2005; Anderson *et al.* 2008; Angeles *et al.* 2014). *Drosophila Bcs1l* ortholog is 60% identical to human. We have generated a *DmBcs1l*$^{p.L78X}$ mutant fly line using the CRISPR/Cas9 technology. We have also found that a broad *Bcs1l* knock-down using RNAi causes pupal lethality and that a homozygous *Bcs1l*$^{p.L78X}$ mutation causes second-instar larval lethality (Rajendran *et al.* unpublished data). These fly strains could be used for cost-effective pharmacological screening as well as mechanistic studies, the results of which can then be verified in the *Bcs1l*$^{p.S78G}$ mice.

Tiivistelmä

GRACILE-oireyhtymä on suomalaiseen tautiperimään kuuluva vaikea vastasyntyneiden mitokondriosairaus, jonka aiheuttaa homotsygoottinen pistemutaatio (*c.A232G*, p.Ser78Gly) *BCS1L*-geenissä. GRACILE-oireyhtymässä mitokondrioiden hengitysketjun kompleksi III (CIII) on viallinen, mikä johtaa vaikeaan aineenvaihdunnan häiriöön, maksa- ja munuaissairauteen ja varhaiseen kuolemaan. Sairauden syntymekanismien ja hoitomahdollisuuksien tutkimuksessa on osoittautunut erittäin hyödylliseksi hiirimalli, jossa potilaiden pistemutaatio on viety hiiren genomiin. Hiirimallissa toistuvat useimmat potilaiden oireet, kuten kasvuhäiriö, alhainen verensokeri ja maksa- ja munuaissairaus. Homotsygoottiset hiiret (*Bcs1l*$^{p.S78G}$) kuolevat C57BL/6JBomTac-kannassa vain 30-40 päivän ikäisinä, todennäköisesti hypoglykemiaan. Sen vuoksi tutkimme tässä väitöskirjassa sokeripitoisen ruoan (60 % glukoosia) vaikutusta hiirten verensokeriin ja elinikään. Sokerilisä johti kuitenkin jopa hiukan lyhempään elinikään huolimatta siitä, että se näytti korjaavan joidenkin aineenvaiduntatuotteiden pitoisuuksia plasmassa. Seuraavissa osatöissä huomasimme, että C57BL/6JCrl-kannassa hiiret elivät viisi kertaa pidempään (noin 200 päivää) kuin aikaisemmin Lundin yliopistossa käytetyssä kannassa, ja niille kehittyi uusia myöhään alkavia oireita kuten vaikea sydänlihassairaus ja aivomuutoksia. Tässä kannassa tutkimme ensin rasvapitoisen (ketogeenisen) ruokavalion vaikutusta maksasairauden etenemiseen. Ketogeenisella ruokavaliolla oli selvä myönteinen vaikutus maksasairaukseen ensimmäisten kolmen kuukauden aikana, mutta pitkäkestoinen ruokinta aiheutti haittavaikutuksia. Kolmannessa osatutkimuksessa risteytimme *Bcs1l*-mutaatiota kantavia hiiriä vaihtoehtoista oksidaasia (AOX) ilmentävän siirtogeenisen hiirilinjan kanssa. AOX voi parantaa hengitysketjun alkuosan toimintaa ohjaamalla esimerkiksi CIII:n toimintahäiriön vuoksi pysähtynyttä elektronien kulkua koentsyymi Q:lta suoraan hapelle. AOX:n esti kokonaan sydänlihassairauden ja munuaissurkastuman kehittymisen *Bcs1l*$^{p.S78G}$-hiirille ja hidasti aivomuutosten etenemistä. Sydänsairauden estymisen johdosta AOX-siirtogeeniä kantavien mutanttihiirten keskimääräinen elinikä piteni 210 päivästä 590:een. Väitöskirjatutkimusten tärkeimpiä johtopäätöksiä ovat, että C57BL/6JCrl-kannassa *Bcs1l*$^{p.S78G}$-hiirillä ilmenee sekä GRACILE-oireyhtymälle tyypillisiä alkuvaiheen oireita, kuten kasvuhäiriö ja maksasairaus, että myöhemmin kehittyviä uusia oireita, kuten sydänlihassairaus, joita esiintyy muissa CIII-puutossairauksissa. Ruokavaliohoidoilla oli edullista vaikutusta maksasairauteen, mutta muutoin vaikutukset olivat vähäisiä tässä vaikean mitokondriosairauden mallissa. Sitä vastoin hengitysketjun pysähtyneen elektronivirtauksen palauttaminen AOX-entsyymin avulla oli ennennäkemättömän tehokas keino hidastaa tai jopa estää pysyvästi vakavia oireita, ja vaikutus oli selvin kudoksissa tai soluissa, joilla on suuri energiankulutus, kuten sydämessä ja munuaisten tubuluksissa.

ஆராட்சியின் சுருக்கம்

என்னுடைய ஆராய்ச்சியானது க்ரஸைல் என்னும் கொடிய மரபு நோயினால் பாதிக்கப்பட்ட மைட்டோகாண்ட்ரியாவின் செயல்பாட்டை மேம்படுத்த சரியான வழிமுறைகளை கண்டறிவதே ஆகும். ஒரு மரபணு பிழை *BCS1L*$^{c.A232G}$, பிறந்த குழந்தைகளில் க்ரஸைல் என்னும் கொடிய நோயை ஏற்படுத்துகிறது. இந்த மரபு நோய் மைட்டோகாண்ட்ரியாவின் சுவாச-சங்கிலி குழுமம் III-இல் கோளாறு ஏற்படுத்துவதின் மூலம் பல உறுப்புக்களை செயலிழக்க செய்து குழந்தைகளில் சிசு பருவத்திலேயே மரணத்தையும் விளைவிக்கிறது. நோய்க்காண மரபணு பிழைடைய எலி மாதிரிகளை பயன்படுத்தி இந்த நோயின் விளைவுகளை கண்டறிந்தோம். இந்த எலிகள் மனிதனில் காணப்படும் அதே நோய் விளைவுகளான வளர்ச்சி கட்டுப்பாடு, கல்லீரல் குறைபாடு, மற்றும் சிறுநீரக நுண்-குழாய் குறைபாடு போன்றவற்றை வளர்த்துக்கொள்கிறன. இந்த நோயானது மனிதர்களிடம் விளைவிப்பது போலவே எலியிலும் வாழ் நாளை குறைக்கிறது (35-45 நாட்கள்). முதலில், இத்தகைய ஆரம்பகால மரணத்திற்கு கடுமையான இரத்தச் சர்க்கரைக் குறைபாடே முதன்மை காரணமாக கண்டறியப்பட்டதால், சர்க்கரையின் சமநிலையை மேம்படுத்துவதற்காக எலிகளுக்கு அதிக சர்க்கரை உடைய (டெக்ஸ்ட்ரோஸ்) உணவை ஊட்டமளித்து ஆய்வு செய்தோம். இந்த உணவு இரத்தத்தில் சில வளர்ச்சிதைப்பொருட்களில் மாற்றம் ஏற்படுத்தியதை தவிர ஆற்றல் வளர்சிதை மாற்றத்தை மேம்படுத்தவில்லை. இந்நோய்காரணியான மரபணு பிழையை மற்றோரு மரபு பின்புலத்தில் C57BL/6JCrl உள்ள எலிகளுக்குள் அறிமுகப்படுத்தியபோது, எலிகளின் வாழ்நாள் முந்தய எலி மாதிரியைக்காட்டிலும் ஐந்து மடங்காக நீட்டித்தது. இந்த வாழ்நாள் நீட்டிப்பு எலிகளிடையே மூளைக்குறைபாடு மற்றும் இருதயத் தசைநோய் போன்ற புதிய குறைபாடு**களை** வெளிக்கொணர்ந்தது. நோய் வளர்ச்சியை கட்டுப்படுத்தும் நோக்கத்துடன், கீட்டோஜென் என்ற அதிக கொழுப்பு கொண்ட உணவை எலிகளுக்கு ஊட்டமளித்து ஆய்வு செய்ததில், கீட்டோஜென் உணவு கல்லீரல் குறைபாட்டை சிறிதளவு கட்டுப்படுத்தியதைக் கண்டறிந்தோம். ஆனால் நீண்ட கால கீட்டோஜென் ஊட்டம் எலிகளின் வாழ் தரத்தையும் மற்றும் நாட்களையும் குறைத்தது. மற்றோரு ஆய்வில், சுவாசச் சங்கிலி செயல்பாட்டை மேம்படுத்த, மரபு பிழையுடைய எலிகளுக்கு கூடுதலாக ஒரு மாற்று ஆக்ஸிடேஸ் என்னும் பரிமாற்ற மரபணுவை அறிமுகப்படுத்தினோம். இதன் புரதமானது குழுமம் III-ன் குறைபாட்டை தவிர்த்து எலக்ட்ரான் பரிமாற்றத்தை மேம்படுத்தக்கூடியது. இந்த மாற்று-ஆக்ஸிடேஸ் புரதம் நோய்வாய்ப்பட்ட எலிகளில் இருதயத்தசைநோய் மற்றும் சிறுநீரக நுண்-குழாய் நலிவு போன்றவற்றை முற்றிலுமாக தவிர்த்ததோடு, மூளையின் சாமட்டோசென்சரி படலத்தில் அஸ்ட்ரோஸைட் அணுக்களின் குவிப்பை தாமதித்தது. மேலும், இந்த புரதம் எலிகளின் வாழ் நாளை சராசரியாக 590 நாட்களாக நீட்டித்தது. எனது ஆய்வுகளின் முக்கிய தீர்மானங்கள் பின் வருவனவையாகும். *Bcs1l*$^{p.S78G}$ மரபணு பிழை ஏற்படுத்தப்பட்ட எலிகள் குழுமம் III குறைபாட்டினால் மனிதனில் ஏற்படும் அனைத்து விளைவுகளையும் கொண்டுள்ளது. மேலும், எலிகளின் கடுமையான வளர்ச்சி கட்டுப்பாட்டின் மேல் எந்தவகையான உணவு மாற்றமும் பெரிதான தாக்கத்தை ஏற்படுத்தவில்லை. மாற்று-ஆக்ஸிடெஸ் புரதமானது இதய மற்றும் சிறுநீரக நுண்ணுயிர்-குழாய் செல்கள் போன்ற உயர் ஏடிபி தேவையுடைய திசுக்கள் அல்லது செல்களில் பயனுள்ளதாக அமைகிறது,

Acknowledgments

First of all, I am grateful to Faculty of Medicine and Doctoral Program in Biomedicine at Helsinki University for the opportunity to pursue my doctoral study. This doctoral thesis work was carried out at the Folkhalsan Research Center and Helsinki University during the year 2014-2018.

Studies compiled in my dissertation were financially supported by several organizations and foundations from multiple countries. They are Lund University (to Vineta Fellman), Swedish research council (to Vineta Fellman), Skane council foundation for research and development (to Vineta Fellman), Distinguished professor award at Karolinska Institute (to Juha Kere), Strategic research program funding on diabetes to Karolinska Institute, European research council (to Howard T Jacobs), German federal ministry of education and research, Academy of Finland (to Vineta Fellman and Howard T Jacobs), Finnish physicians society (to Vineta Fellman), Foundation for Pediatric research in Finland (to Vineta Fellman), University of Helsinki travel grant (to Jayasimman Rajendran), Juhani Aho Foundation of Medical Research (Jayasimman Rajendran), and Folkhälsan Research Center (to Vineta Fellman and Jukka Kallijärvi).

I would like to thank Professor Markku Heikinheimo for serving as custos for my public examination. I thank Professor Cristina Ugalde for being opponent and my reviewers Docent Alexander Kastaniotis and Docent Riikka Martikainen for providing valuable suggestions to improve my dissertation.

I would like to thank my primary supervisor Professor Vineta Fellman for introducing me to the field of mitochondrial research. I thank Vineta for providing the opportunity to do my doctoral thesis in her group. Your encouragement and support motivated me to discover the novel findings such as survival difference and cardiomyopathy in our mouse model, which are the base discovery for other ongoing research studies in our group. I thank you for the motivation and opportunity you provide me to travel and attend the scientific meetings in the mitochondrial research world. Your strict deadlines and constructive feedbacks were successful to complete my study in time. I am thankful to Dr.Jukka Kallijärvi for the opportunity to work under his supervision and also providing an atmosphere to work as an independent researcher. Thank you for recognizing my talents and skills, and putting it to its best use in collaborative projects as well. Again, I thank Vineta and Jukka for their advice on writing this thesis; it would not have been completed without your support.

I am thankful to my thesis follow-up committee members Dr. Alberto Sanz and Associate professor Henna Tyynismaa for monitoring my progress every year. Your valuable comments and support helped me to stay focused on the aims of my thesis.

I would like to thank my fellow Ph.D. student Janne Purhonen for sharing his practical experience and providing ideas for troubleshooting the experiments. I wish good luck to your doctoral study and future career. I thank our technical assistant Elisa Altay for her excellent assistance in the laboratory work. You were supportive and created a lively atmosphere at work. I thank you for being a good friend and sharing experience of archery class and chess game.

I would like to thank our former colleagues and co-authors from Lund University Nikica Tomašić, Dr. Heike Kotarsky and Eva Hansson for their input in my research. I thank you all including Dr. Mina Davoudi for familiarizing me to the behavioral characteristics of our mouse model and sharing experience of blue-native PAGE. I am grateful to you all for the hospitality during my stay at Lund University. I thank former colleagues and co-authors Dr. Saara Tegelberg and Dr. Kristina Uusi-Ruva for their inputs, though we work together for a short time, your input for our research was significant.

I thank all the collaborators and co-authors mentioned in the original publication for their contributions to laboratory experiments and writing. I thank Dr. Howard T. Jacobs and Dr. Marten Szibor for their support and knowledge provided for our AOX project. Your valuable comments and discussions helped to build our manuscript stronger. I thank Praveen Kumar Dhandapani for our break time scientific discussions on AOX project and your support as a friend.

I thank Päivi Leinikka for sharing echocardiography, Tuula Manninen for sharing knowledge on CLAMs, Jatin Nandania for running metabolomics analysis, Dr. Eero Mervala and Dr. Hannu Sariola for advice on the heart and kidney assessment respectively, Dr. Eric Dufour for advice on respirometry, and Nada Bechara-Hirvonen for blood chemistry analysis. I thank former students Vlad and Vilma for being supportive and sharing entire work experience with me. I wish best for their future career. I thank scientists, collaborators, and members of the German mouse clinic for their contributions in the extensive animal phenotyping and their written report.

I thank Sajan Raju and his (FinHit) group members for our fun and laughs during lunch break. I am grateful to all the members and friends working at Folkhälsan Research Center for memorable times that we had together in the lab parties and scientific-day meetings. I thank head technicians of Folkhälsan Research Center, Ann-Liz and Teija for their support in inventory management and animal work, respectively. I thank Dr. Peter Heckman for arranging my seminar session in the

Thursday meetings for every year and exhibit my work progress to fellow researchers. I thank Folkhälsan management for taking care of all the documentation regarding my work contracts and financial arrangements.

I thank all my friends around the world for their support during these years of my study. Special thanks to Boobalan and Sharan for their encouragement. I thank my former supervisor from my Master's degree, Dr. Micheal J Williams for his early guidance and constant motivation for my scientific career.

I am grateful to my parents Rajendran and Kala Valli for their love and support. You always believe in me that one day I will reach my goal. I thank my siblings Aparajithan and Shreemathy for their love and encouragement. I express my gratitude my extended family, my Mother-in-law Meera Rai and brother-in-law Nishant for their love and accepting me as a part of the family.

Finally, I am indebted to my wife Neha for her love, support, encouragement, and for being patient with me. Thank you for being supportive at my hard times. I love you.

Helsinki, February 2019

References

Ahola-Erkkilä S, *et al.* 2010. Ketogenic diet slows down mitochondrial myopathy progression in mice. *Human Molecular Genetics*, 19(10), pp.1974–1984.

Al-Owain M *et al.* 2013. Clinical and biochemical features associated with BCS1L mutation. *J Inherit Metab Dis*, 36(813), pp.1573–2665.

Ames BN, 1983. Dietary carcinogens and anticarcinogens. *Science*, 221(4617), p.1256 LP-1264.

Amirsadeghi S, *et al.* 2006. Changes in plant mitochondrial electron transport alter cellular levels of reactive oxygen species and susceptibility to cell death signaling molecules. *Plant and Cell Physiology*, 47(11), pp.1509–1519.

Anderson PR, *et al.* 2008. Hydrogen peroxide scavenging rescues frataxin deficiency in a Drosophila model of Friedreich's ataxia. *Proceedings of the National Academy of Sciences*, 105(2), pp.611–616.

Angeles DC, *et al.* 2014. Thiol peroxidases ameliorateLRRK2mutant-induced mitochondrial and dopaminergic neuronal degeneration in Drosophila. *Human Molecular Genetics*, 23(12), pp.3157–3165.

Antico Arciuch VG, *et al*. 2012. Mitochondrial Regulation of Cell Cycle and Proliferation. *Antioxidants & Redox Signaling*, 16(10), pp.1150–1180.

Antonicka H, *et al.* 2003a. Mutations in COX10 result in a defect in mitochondrial heme A biosynthesis and account for multiple, early-onset clinical phenotypes associated with isolated COX deficiency. *Human Molecular Genetics*, 12(20), pp.2693–2702.

Antonicka H, *et al.* 2003b. Mutations in COX15 Produce a Defect in the Mitochondrial Heme Biosynthetic Pathway, Causing Early-Onset Fatal Hypertrophic Cardiomyopathy. *The American Journal of Human Genetics*, 72(1), pp.101–114.

Avula S, *et al.* 2014. Treatment of Mitochondrial Disorders. *Curr Treat Options neurol.*, 16(6), p.292.

Bahr JT & Bonner WD. 1973. Cyanide-insensitive Respiration: The steady states of skunk cabbage spadix and bean hypocotyl mitochondria. *The Journal of biological chemistry*, 248(10), pp.3441–3446

Barel O, *et al.* 2008. Mitochondrial Complex III Deficiency Associated with a Homozygous Mutation in UQCRQ. *American Journal of Human Genetics*, 82(5), pp.1211–1216.

Bartolák-Suki E, *et al.* 2017. Regulation of mitochondrial structure and dynamics by the cytoskeleton and mechanical factors. *International Journal of Molecular Sciences*, 18(8), pp.7–11.

Berger I, *et al.* 2008. Mitochondrial complex I deficiency caused by a deleterious NDUFA11 mutation. *Annals of Neurology*, 63(3), pp.405–408.

Blázquez A, Gil-Borlado MC, Morán M, *et al.* 2009. Infantile mitochondrial encephalomyopathy with unusual phenotype caused by a novel *BCS1L* mutation in an isolated complex III-deficient patient. *Neuromuscular Disorders*, 19(2), pp.143–146.

Boison D, 2017. New insights into the mechanisms of the ketogenic diet. *Current Opinion in Neurology*, 30(2), pp.187-192.

Cecchini G, 2003. Function and Structure of Complex II of the Respiratory Chain. *Annual Review of Biochemistry*, 72(1), pp.77–109.

Cerutti R, *et al.* 2014. NAD+-dependent activation of Sirt1 corrects the phenotype in a mouse model of mitochondrial disease. *Cell Metabolism*, 19(6), pp.1042–1049.

Chaudhuri M, Ott RD, and Hill GC, 2006. Trypanosome alternative oxidase: from molecule to function. *Trends in Parasitology*, 22(10), pp.484–491.

Clanton RM, *et al.* 2017. Control of seizures by ketogenic diet-induced modulation of metabolic pathways. *Amino Acids*, 49(1), pp.1–20.

Crespo MJ, *et al.* 2008. Cardiac Oxidative Stress Is Elevated at the Onset of Dilated Cardiomyopathy in Streptozotocin-Diabetic Rats. *Journal of Cardiovascular Pharmacology*

and Therapeutics, 13(1), pp.64–71.
Crofts AR, *et al.* 2017. The Q-Cycle Mechanism of the bc1 Complex: A Biologist's Perspective on Atomistic Studies. *The Journal of Physical Chemistry B*, 121(15), pp.3701–3717.
Cruciat CM, *et al.* 1999. Bcs1p, an AAA-family member, is a chaperone for the assembly of the cytochrome bc1complex. *EMBO Journal*, 18(19), pp.5226–5233.
Cvetkovska M, & Vanlerberghe GC. 2012. Alternative oxidase modulates leaf mitochondrial concentrations of superoxide and nitric oxide. *New Phytologist*, 195(1), pp.32–39.
Dabrowska A, *et al.* 2015. PGC-1α controls mitochondrial biogenesis and dynamics in lead-induced neurotoxicity. *Aging*, 7(9), pp.1–19.
Dassa EP, *et al.* 2009. Expression of the alternative oxidase complements cytochrome c oxidase deficiency in human cells. *EMBO Molecular Medicine*, 1(1), pp.30–36.
Davoudi M, *et al.* 2014. Complex I function and supercomplex formation are preserved in liver mitochondria despite progressive complex III deficiency. *PLoS ONE*, 9(1). e86767.
Davoudi M, et al. 2016. COX7A2L / SCAFI and Pre-Complex III Modify Respiratory Chain Supercomplex Formation in Different Mouse Strains with a Bcs1l Mutation. *PLoS ONE*, 11(12), pp.1–11.
Dogan SA, *et al.* 2018. Perturbed Redox Signaling Exacerbates a Mitochondrial Myopathy. *Cell Metabolism*, 28, pp.1–12.
Du D, Shi YH, and Le GW. 2010. Oxidative stress induced by high-glucose diet in liver of C57BL/6J mice and its underlying mechanism. *Molecular Biology Reports*, 37(8), pp.3833–3839
El-Hattab AW, *et al.* 2017. Therapies for mitochondrial diseases and current clinical trials. *Molecular Genetics and Metabolism*, 122(3), pp.1–9.
Endo T & Kohda D. 2002. Functions of outer membrane receptors in mitochondrial protein import. *Biochimica et Biophysica Acta (BBA)*, 1592(1), pp.3–14.
Falco M, *et al.* 2017. Novel compound heterozygous mutations in BCS1L gene causing Bjornstad syndrome in two siblings. *American Journal of Medical Genetics Part A*, 173(5), pp.1348–1352.
Fellman V, *et al.* 1998. Iron-overload disease in infants involving fetal growth retardation, lactic acidosis, liver haemosiderosis, and aminoaciduria. *Lancet*, 351(9101), pp.490–493.
Fellman V, *et al.* 2008. Screening of BCS1L mutations in severe neonatal disorders suspicious for mitochondrial cause. *Journal of Human Genetics*, 53(6), pp.554–558.
Fellman V. 2002. The GRACILE Syndrome, a Neonatal Lethal Metabolic Disorder with Iron Overload. *Blood Cells, Molecules, and Diseases*, 29(3), pp.444–450.
Fernandez-Ayala DJM, *et al.* 2009. Expression of the Ciona intestinalis Alternative Oxidase (AOX) in Drosophila Complements Defects in Mitochondrial Oxidative Phosphorylation. *Cell Metabolism*, 9(5), pp.449–460.
Fernandez-Moreira D, *et al.* 2007. X-linked NDUFA1 gene mutations associated with mitochondrial encephalomyopathy. *Annals of Neurology*, 61(1), pp.73–83.
Fernandez-Vizarra E, *et al.* 2007. Impaired complex III assembly associated with BCS1L gene mutations in isolated mitochondrial encephalopathy. *Human Molecular Genetics*, 16(10), pp.1241–1252.
Fernández-Vizarra E, Tiranti V, and Zeviani M. 2009. Assembly of the oxidative phosphorylation system in humans: What we have learned by studying its defects. *Biochimica et Biophysica Acta - Molecular Cell Research*, 1793(1), pp.200–211.
Fernandez-Vizarra E, and Zeviani M. 2018. Mitochondrial complex III Rieske Fe-S protein processing and assembly Mitochondrial complex III Rieske Fe-S protein processing and assembly. *Cell Cycle*, 17(6), pp.681–687.
Frank KF, *et al.* 2003. Sarcoplasmic reticulum Ca2+ -ATPase modulates cardiac contraction and relaxation. *Cardiovascular Research*, 57, pp.20–27.

Friedrich T, and Böttcher B. 2004. The gross structure of the respiratory complex I: A Lego System. *Biochimica et Biophysica Acta - Bioenergetics*, 1608(1), pp.1–9.
Ghezzi D, *et al.* 2008. FASTKD2 Nonsense Mutation in an Infantile Mitochondrial Encephalomyopathy Associated with Cytochrome C Oxidase Deficiency. *American Journal of Human Genetics*, 83(3), pp.415–423.
Ghezzi D, *et al.* 2011. Mutations in TTC19 cause mitochondrial complex III deficiency and neurological impairment in humans and flies. *Nature genetics*, 43(3), pp.259–263.
Gil-Borlado MC, *et al.* 2009. Pathogenic mutations in the 5' untranslated region of BCS1L mRNA in mitochondrial complex III deficiency. *Mitochondrion*, 9(5), pp.299–305.
Gregory KN, *et al.* 2006. Histidine-rich Ca binding protein: regulator of sarcoplasmic reticulum calcium sequestration and cardiac function. *Journal of Molecular and Cellular Cardiology*, 40(5), pp.653–665.
Guo R, *et al.* 2018. Structure and mechanism of mitochondrial electron transport chain. *Biomedical Journal*, 41(1), pp.9–20.
Gupta KJ, Igamberdiev AU, and Mur LAJ. 2012. NO and ROS homeostasis in mitochondria: A central role for alternative oxidase. *New Phytologist*, 195(1), pp.1–3.
Gupta RC, *et al.* 1997. SR Ca(2+)-ATPase activity and expression in ventricular myocardium of dogs with heart failure. *American Journal of Physiology-Heart and Circulatory Physiology*, 273(1), pp.H12–H18.
Hagen CM, *et al.* 2013. *MT-CYB* mutations in hypertrophic cardiomyopathy. *Molecular Genetics & Genomic Medicine*, 1(1), pp.54–65.
Hakkaart G, *et al.* 2006. Allotopic expression of a mitochondrial alternative oxidase confers cyanide resistance to human cell respiration. *EMBO reports*, 7(3), pp.341–345.
Hellemond JJ Van, *et al.* 2007. A Gene Encoding the Plant-Like Alternative Oxidase is Present in Phytomonas but Absent in Leishmania spp. *Journal of Eukaryotic Microbiology*, 45(4), pp.426–430.
Hes FJ, *et al.* 2010. Low penetrance of a SDHB mutation in a large Dutch paraganglioma family. *BMC Medical Genetics*, 11(1), pp.1–5.
van den Heuvel L, *et al.* 1998. Demonstration of a new pathogenic mutation in human complex I deficiency: a 5-bp duplication in the nuclear gene encoding the 18-kD (AQDQ) subunit. *American journal of human genetics*, 62(2), pp.262–8.
Hinson JT, *et al.* 2007. Missense Mutations in the BCS1L Gene as a Cause of the Björnstad Syndrome. *The new england journal of medicine*, 356(8), pp.809–819.
Hirst J, *et al.* 2003. The nuclear-encoded subunits of complex I from bovine heart mitochondria. *Biochimica et Biophysica Acta - Bioenergetics*, 1604(3), pp.135–150.
Hoefs SJG, *et al.* 2008. NDUFA2 Complex I Mutation Leads to Leigh Disease. *American Journal of Human Genetics*, 82(6), pp.1306–1315.
Hoefs SJG, *et al.* 2011. NDUFA10 mutations cause complex i deficiency in a patient with Leigh disease. *European Journal of Human Genetics*, 19(3), pp.270–274.
Hoekstra AS and Bayley JP. 2013. The role of complex II in disease. *Biochimica et Biophysica Acta - Bioenergetics*, 1827(5), pp.543–551.
Hoogenraad NJ, Ward LA, and Ryan MT. 2002. Import and assembly of proteins into mitochondria of mammalian cells. *Biochimica et Biophysica Acta - Molecular Cell Research*, 1592(1), pp.97–105.
Howard, CF. 1970. Synthesis of Fatty Acids in Outer and Inner Membranes of Mitochondria. *The Journal of biological chemistry*, 245(10), pp.462–468.
Humphrey DM *et al.* 2012. Alternative oxidase rescues mitochondria-mediated dopaminergic cell loss in Drosophila. *Human Molecular Genetics*, 21(12), pp.2698–2712.
Jacobs HT, *et al.* 2004. Mitochondrial disease in flies. *Biochimica et Biophysica Acta - Bioenergetics*, 1659(2–3), pp.190–196.

Jastroch M, *et al.* 2010. Mitochondrial proton and electron leaks. *Essays Biochem*, 47, pp.53–67.
Kang HC, *et al.* 2007. Safe and Effective Use of the Ketogenic Diet in Children with Epilepsy and Mitochondrial Respiratory Chain Complex Defects. *Epilepsia*, 48(1), pp.82–88.
Kasapkara ÇS, *et al.* 2014. BCS1L gene mutation causing GRACILE syndrome: Case report. *Renal Failure*, 36(6), pp.953–954.
Kemppainen KK, *et al.* 2014. Expression of alternative oxidase in Drosophila ameliorates diverse phenotypes due to cytochrome oxidase deficiency. *Human Molecular Genetics*, 23(8), pp.2078–2093.
Kennedy AR, *et al.* 2007. A high-fat, ketogenic diet induces a unique metabolic state in mice. *AJP: Endocrinology and Metabolism*, 292(6), pp.E1724–E1739.
Khan NA, *et al.* 2014. Effective treatment of mitochondrial myopathy by nicotinamide riboside, a vitamin B3. *EMBO Molecular Medicine*, 6(6), pp.721–731.
Kim DY and Rho JM. 2008. The ketogenic diet and epilepsy. *Current Opinion in Clinical Nutrition & Metabolic Care*, 11(2), pp.113-120.
Kirby DM, *et al.* 2004. NDUFS6 mutations are a novel cause of lethal neonatal mitochondrial complex I deficiency. *Journal of Clinical Investigation*, 114(6), pp.837–845.
Koga Y, Arika Y, and Nishioka J. 2005. L -Arginine improves the symptoms of strokelike episodes in MELAS. *Neurology*, 64, pp.710–712.
Kotarsky H, *et al.* 2012. Metabolite profiles reveal energy failure and impaired beta-oxidation in liver of mice with complex iii deficiency due to a bcs1l mutation. *PLoS ONE*, 7(7), pp.1–10.
Lazarou M, *et al.* 2009. Assembly of mitochondrial complex I and defects in disease. *Biochimica et Biophysica Acta - Molecular Cell Research*, 1793(1), pp.78–88.
Levéen P, *et al.* 2011. The GRACILE mutation introduced into Bcs1l causes postnatal complex III deficiency: A viable mouse model for mitochondrial hepatopathy. *Hepatology*, 53(2), pp.437–447.
Li S, *et al.* 2012. Intracellular alkalinization induces cytosolic Ca2+increases by inhibiting sarco/endoplasmic reticulum Ca2+-ATPase (SERCA). *PLoS ONE*, 7(2), p.e31905.
de Lonlay P, *et al.* 2001. A mutant mitochondrial respiratory chain assembly protein causes complex III deficiency in patients with tubulopathy, encephalopathy and liver failure. *Nat Genet*, 29(1), pp.57–60.
Lynn AM, *et al.* 2012. BCS1L gene mutation presenting with GRACILE-like syndrome and complex III deficiency. *Annals of Clinical Biochemistry*, 49(2), pp.201–203.
Maio N, *et al.* 2017. A Single Adaptable Cochaperone-Scaffold Complex Delivers Nascent Iron-Sulfur Clusters to Mammalian Respiratory Chain Complexes I–III. *Cell Metabolism*, 25(4), p.945–953.
Maio N, *et al.* 2014. Cochaperone binding to LYR motifs confers specificity of iron-sulfur cluster delivery. *Cell Metabolism*, 19(3), pp.445–457.
Martin WF, Garg S, and Zimorski V. 2015. Endosymbiotic theories for eukaryote origin. *Philosophical Transactions of the Royal Society B: Biological Sciences*, 370(1678), e20140330.
Matsa LS, *et al.* 2013. Haplotypes of NOS3 Gene Polymorphisms in Dilated Cardiomyopathy. *PLoS ONE*, 8(7), pp.1–5.
Maxwell DP, Wang Y, and McIntosh L. 1999. The alternative oxidase lowers mitochondrial reactive oxygen production in plant cells. *Proceedings of the National Academy of Sciences*, 96(14), pp.8271–8276.
McBride HM, Neuspiel M, and Wasiak S. 2006. Mitochondria: More Than Just a Powerhouse. *Current Biology*, 16(14), pp.551–560.
McDonald AE and Vanlerberghe GC. 2004. Branched mitochondrial electron transport in the animalia: Presence of alternative oxidase in several animal phyla. *IUBMB Life*, 56(6), pp.333–341.

McDonald AE and Vanlerberghe GC. 2006. Origins, evolutionary history, and taxonomic distribution of alternative oxidase and plastoquinol terminal oxidase. *Comparative Biochemistry and Physiology Part D: Genomics and Proteomics*, 1(3), pp.357–364.

McDonald AE, Vanlerberghe GC, and Staples JF. 2009. Alternative oxidase in animals: unique characteristics and taxonomic distribution. *Journal of Experimental Biology*, 212(16), pp.2627–2634.

De Meirleir L, *et al.* 2003. Clinical and diagnostic characteristics of complex III deficiency due to mutations in the BCS1L gene. *American journal of medical genetics. Part A*, 121A(2), pp.126–31.

Di Meo I, *et al.* 2012. Effective AAV-mediated gene therapy in a mouse model of ethylmalonic encephalopathy. *EMBO Molecular Medicine*, 4(9), pp.1008–1014.

Mermigkis C, *et al.* 2013. Medical treatment with thiamine, coenzyme Q, vitamins e and C, and carnitine improved obstructive sleep apnea in an adult case of Leigh disease. *Sleep and Breathing*, 17(4), pp.1129–1135.

Meunier B, *et al.* 2013. Respiratory complex III dysfunction in humans and the use of yeast as a model organism to study mitochondrial myopathy and associated diseases. *Biochimica et Biophysica Acta - Bioenergetics*, 1827(11–12), pp.1346–1361.

Millar A and Day D. 1996. Nitric oxide inhibits the cytochrome oxidase but not the alternative oxidase of plant mitochondria. *FEBS letters*, 398, pp.155–158.

Mimaki M, *et al.* 2012. Understanding mitochondrial complex I assembly in health and disease. *Biochimica et Biophysica Acta - Bioenergetics*, 1817(6), pp.851–862.

Mingozzi F and High KA. 2011. Therapeutic in vivo gene transfer for genetic disease using AAV: Progress and challenges. *Nature Reviews Genetics*, 12(5), pp.341–355.

Moran M, *et al.* 2010. Cellular pathophysiological consequences of BCS1L mutations in mitochondrial complex III enzyme deficiency. *Human Mutation*, 31(8), pp.930–941.

Mordaunt DA, *et al.* 2015. Phenotypic variation of TTC19-deficient mitochondrial complex III deficiency: A case report and literature review. *American Journal of Medical Genetics, Part A*, 167(6), pp.1330–1336.

Murphy MP. 2009. How mitochondria produce reactive oxygen species. *The Biochemical journal*, 417(1), pp.1–13.

Neergheen V, *et al.* 2017. Coenzyme Q 10 in the Treatment of Mitochondrial Disease. *Journal of Inborn Errors of Metabolism and Screening*, 5, pp.1–8.

Nightingale H, *et al.* 2016. Emerging therapies for mitochondrial disorders. *Brain*, 139(6), pp.1633–1648.

Norio R. 2003. Finnish Disease Heritage II:population prehistory and genetic roots of Finns. *Hum Genet*, 112(5-6), pp.457-469.

Nouet C, *et al.* 2009. Functional Analysis of Yeast bcs1 Mutants Highlights the Role of Bcs1p-Specific Amino Acids in the AAA Domain. *Journal of Molecular Biology*, 388(2), pp.252–261.

Ogawa Y. 1994. Role of Ryanodine Receptors. *Critical Reviews in Biochemistry and Molecular Biology*, 29(4), pp.229–274.

Ozben T. 2007. Oxidative stress and apoptosis: Impact on cancer therapy. *Journal of Pharmaceutical Sciences*, 96(9), pp.2181–2196.

Palsdottir H, *et al.* 2003. Structure of the yeast cytochrome bc1 complex with a hydroxyquinone anion Qo site inhibitor bound. *Journal of Biological Chemistry*, 278(33), pp.31303–31311.

Parikh S, *et al.* 2009. A Modern Approach to the Treatment of Mitochondrial Disease. *Curr Treat Options neurol.*, 11(6), pp.414–430.

Perales-Clemente E, *et al.* 2008. Restoration of electron transport without proton pumping in mammalian mitochondria. *Proceedings of the National Academy of Sciences*, 105(48), pp.18735–18739.

Puigserver P and Spiegelman BM. 2003. Peroxisome proliferator-activated receptor-γ coactivator 1α (PGC-1α): Transcriptional coactivator and metabolic regulator. *Endocrine Reviews*, 24(1), pp.78–90.

Ramos-Arroyo MA, *et al.* 2009. Clinical and biochemical spectrum of mitochondrial complex III deficiency caused by mutations in the BCS1L gene. *Clinical Genetics*, 75(6), pp.585–587.

Rhoads DM, *et al.* 1998. Regulation of the Cyanide-resistant Alternative Oxidase of. *the Journal of Biological Chemistry*, 273(46), pp.30750–30756.

Royo B, *et al.* 2015. Nitric oxide induces the alternative oxidase pathway in Arabidopsis seedlings deprived of inorganic phosphate. *Journal of Experimental Botany*, 66(20), pp.6273–6280.

Sanz A, *et al.* 2010. Expression of the yeast NADH dehydrogenase Ndi1 in Drosophila confers increased lifespan independently of dietary restriction. *Proceedings of the National Academy of Sciences*, 107(20), pp.9105–9110.

Sardiello M, *et al.* 2003. MitoDrome: A database of Drosophila melanogaster nuclear genes encoding proteins targeted to the mitochondrion. *Nucleic Acids Research*, 31(1), pp.322–324.

Schägger H. 2001. Respiratory chain supercomplexes. *IUBMB life*, 52(3–5), pp.119–128.

Schieber M and Chandel NS. 2014. ROS function in redox signaling and oxidative stress. *Current Biology*, 24(10), pp.R453–R462.

Searles CD. 2002. The nitric oxide pathway and oxidative stress in heart failure. *Congest Heart Fail*, 8(3), p.142–147,155.

Serdaroğlu E, *et al.* 2016. A Turkish bcs1l mutation causes gracile-like disorder. *The Turkish Journal of Pediatrics*, 58(6), p.658.

Shi X, *et al.* 2008. Paradoxical effect of mitochondrial respiratory chain impairment on insulin signaling and glucose transport in adipose cells. *Journal of Biological Chemistry*, 283(45), pp.30658–30667.

Shiba T, *et al.* 2013. Structure of the trypanosome cyanide-insensitive alternative oxidase. *Proceedings of the National Academy of Sciences*, 110(12), pp.4580–4585.

Siddiqi S, *et al.* 2013. Novel mutation in AAA domain of BCS1L causing Bjornstad syndrome. *Journal of Human Genetics*, 58(12), pp.819–821.

Sofou K, *et al.* 2017. Ketogenic diet in pyruvate dehydrogenase complex deficiency: short- and long-term outcomes. *Journal of Inherited Metabolic Disease*, 40(2), pp.237–245.

Solis DC, *et al.* 2009. Penetrance and clinical consequences of a gross SDHB deletion in a large family. *Clin Genet*, 75(4), pp.354–363.

Son Y, *et al.* 2011. Mitogen-Activated Protein Kinases and Reactive Oxygen Species : How Can ROS Activate MAPK Pathways ? *Journal of Signal Transduction*, 2011, pp.1–6.

Suzuki T, *et al.* 2004. Direct evidence for cyanide-insensitive quinol oxidase (alternative oxidase) in apicomplexan parasite Cryptosporidium parvum: phylogenetic and therapeutic implications. *Biochemical and Biophysical Research Communications*, 313(4), pp.1044–1052.

Szibor M, *et al.* 2016. Broad AOX expression in a genetically tractable mouse model does not disturb normal physiology. *Disease Models & Mechanisms*, 10(2), pp.163–171.

Taanman J. 1999. The mitochondrial genome: structure, transcription, translation and replication. *Biochimica et Biophysica Acta (BBA)*, 1410, pp.103–123.

Tegelberg S, *et al.* 2017. Respiratory chain complex III deficiency due to mutated BCS1L : a novel phenotype with encephalomyopathy , partially phenocopied in a Bcs1l mutant mouse model. *Orphanet Journal of Rare Diseases*, 12(73), pp.1–14.

Torres-Torronteras J, *et al.* 2014. Gene therapy using a liver-targeted AAV vector restores nucleoside and nucleotide homeostasis in a murine model of MNGIE. *Molecular Therapy*, 22(5), pp.901–907.

Tripoli G, *et al.* 2005. Comparison of the oxidative phosphorylation (OXPHOS) nuclear genes in the genomes of Drosophila melanogaster, Drosophila pseudoobscura and Anopheles gambiae. *Genome Biology*, 6(2), p.R11.

Tuppen HAL, *et al.* 2010. Long-term survival of neonatal mitochondrial complex III deficiency associated with a novel *BCS1L* gene mutation. *Molecular Genetics and Metabolism* , 100(4), pp.345–348.

Udhayabanu T, *et al.* 2017. Riboflavin Responsive Mitochondrial Dysfunction in Neurodegenerative Diseases. *Journal of Clinical Medicine*, 6(5), p.52.

Vanlerberghe GC. 2013. Alternative Oxidase : A Mitochondrial Respiratory Pathway to Maintain Metabolic and Signaling Homeostasis during Abiotic and Biotic Stress in Plants. *Int. J. Mol. Sci.*, 14, pp.6805–6847.

Vanlerberghe GC, *et al.* 1995. Alternative Oxidase Activity in Tobacco Leaf Mitochondria (Dependence on Tricarboxylic Acid Cycle-Mediated Redox Regulation and Pyruvate Activation). *Plant physiology*, 109(2), pp.353–361.

Veiga A, Arrabaça JD, and Loureiro-Dias MC. 2003. Cyanide-resistant respiration, a very frequent metabolic pathway in yeasts. *FEMS Yeast Research*, 3(3), pp.239–245.

Visapää I, *et al.* 2002. GRACILE Syndrome, a Lethal Metabolic Disorder with Iron Overload, Is Caused by a Point Mutation in BCS1L. *The American Journal of Human Genetics*, 71(4), pp.863–876.

Viscomi C, *et al.* 2010. Combined treatment with oral metronidazole and N-acetylcysteine is effective in ethylmalonic encephalopathy. *Nature Medicine*, 16(8), pp.869–871.

Viscomi C, *et al.* 2011. In vivo correction of COX deficiency by activation of the AMPK/PGC-1α axis. *Cell Metabolism*, 14(1), pp.80–90.

Vogel RO, Smeitink JAM, and Nijtmans LGJ. 2007. Human mitochondrial complex I assembly: A dynamic and versatile process. *Biochimica et Biophysica Acta - Bioenergetics*, 1767(10), pp.1215–1227.

Wagener N, *et al.* 2011. A pathway of protein translocation in mitochondria mediated by the AAA-ATPase Bcs1. *Molecular Cell*, 44(2), pp.191–202.

Wagener N and Neupert W. 2012. Bcs1, a AAA protein of the mitochondria with a role in the biogenesis of the respiratory chain. *Journal of Structural Biology*, 179(2), pp.121–125.

Wallace DC, Fan W, and Procaccio V. 2010. Mitochondrial Energetics and Therapeutics. *Annu Rev Pathol*, 5, pp.297–348.

Wang A, *et al.* 2016. Rapamycin enhances survival in a Drosophila model of mitochondrial disease. *Oncotarget*, 7(49), pp.80131–80139.

Wasilewski M, Chojnacka K, and Chacinska A. 2017. Protein trafficking at the crossroads to mitochondria. *Biochimica et Biophysica Acta - Molecular Cell Research*, 1864(1), pp.125–137.

Weraarpachai W, *et al.* 2009. Mutation in TACO1, encoding a translational activator of COX I, results in cytochrome c oxidase deficiency and late-onset Leigh syndrome. *Nature Genetics*, 41, p.833.

Wright DJ, *et al.* 2015. N-Acetylcysteine improves mitochondrial function and ameliorates behavioral deficits in the R6/1 mouse model of Huntington's disease. *Translational Psychiatry*, 5(1), pp.e492-10.

Xiao F, *et al.* 2014. Role of mitochondrial electron transport chain dysfunction in Cr(VI)-induced cytotoxicity in L-02 hepatocytes. *Cellular Physiology and Biochemistry*, 33(4), pp.1013–1025.

Ylikallio E and Suomalainen A. 2012. Mechanisms of mitochondrial diseases. *Annals of Medicine*, 44(1), pp.41–59.

Zhang J, *et al.* 2015. Exome sequencing reveals novel BCS1L mutations in siblings with hearing loss and hypotrichosis. *Gene*, 566(1), pp.84–88.

Zhu Z, *et al.* 1998. SURF1, encoding a factor involved in the biogenesis of cytochrome c oxidase, is mutated in Leigh syndrome. *Nature Genetics*, 20, p.337.

Zieliński ŁP, *et al.* 2016. Metabolic flexibility of mitochondrial respiratory chain disorders predicted by computer modeling. *Mitochondrion*, 31, pp.45–55.